In silico plasmas under extreme conditions: from particle accelerators to pair plasmas in pulsars

Luís O. Silva

@luis_os http://epp.ist.utl.pt/los/

GoLP

Instituto de Plasmas e Fusão Nuclear

Instituto Superior Técnico

Lisbon, Portugal

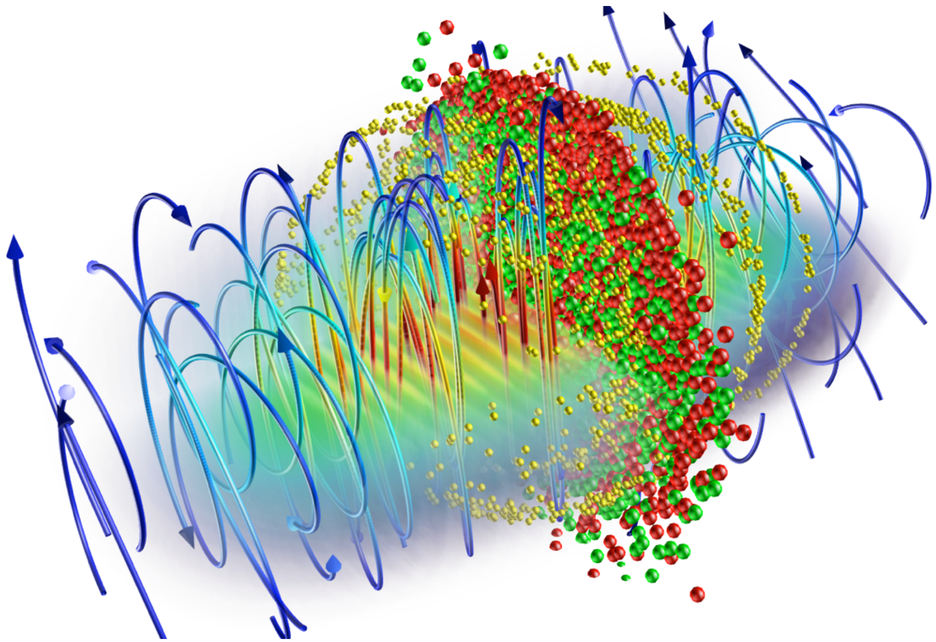

GoLP/IPFN Instituto Superior Técnico

TÉCNICO LISBOA

golp grupo de lasers e plasmas

Acknowledgments

- **R. Fonseca, J. Vieira, T. Grismayer, K. Schoeffler, M. Vranic, J. L. Martins, U. Sinha, N. Shukla, F. Cruz, P. Carneiro**
- Work in collaboration with:
  - **W. B. Mori (UCLA), G. Sarri (QUB), P. Norreys (Oxford)**
- Simulation results obtained at **the Accelerates Cluster (IST), Dawson2 (UCLA), Jugene/Juqueen (FZ Jülich), SuperMUC (Münich), Sequoia (LLNL)**

Advanced Grants "Accelerates" (2010) and InPairs (2015)

Overarching motivation

Many extreme plasma physics scenarios (field intensities in excess of 10^{23} W/cm^2 in the laboratory or in astrophysics) can only be fully explored *in silico*

Several fundamental questions on plasma physics under extreme conditions can now be answered with *ab initio* petascale simulations + theory + experiments with intense beams

http://epp.ist.utl.pt/

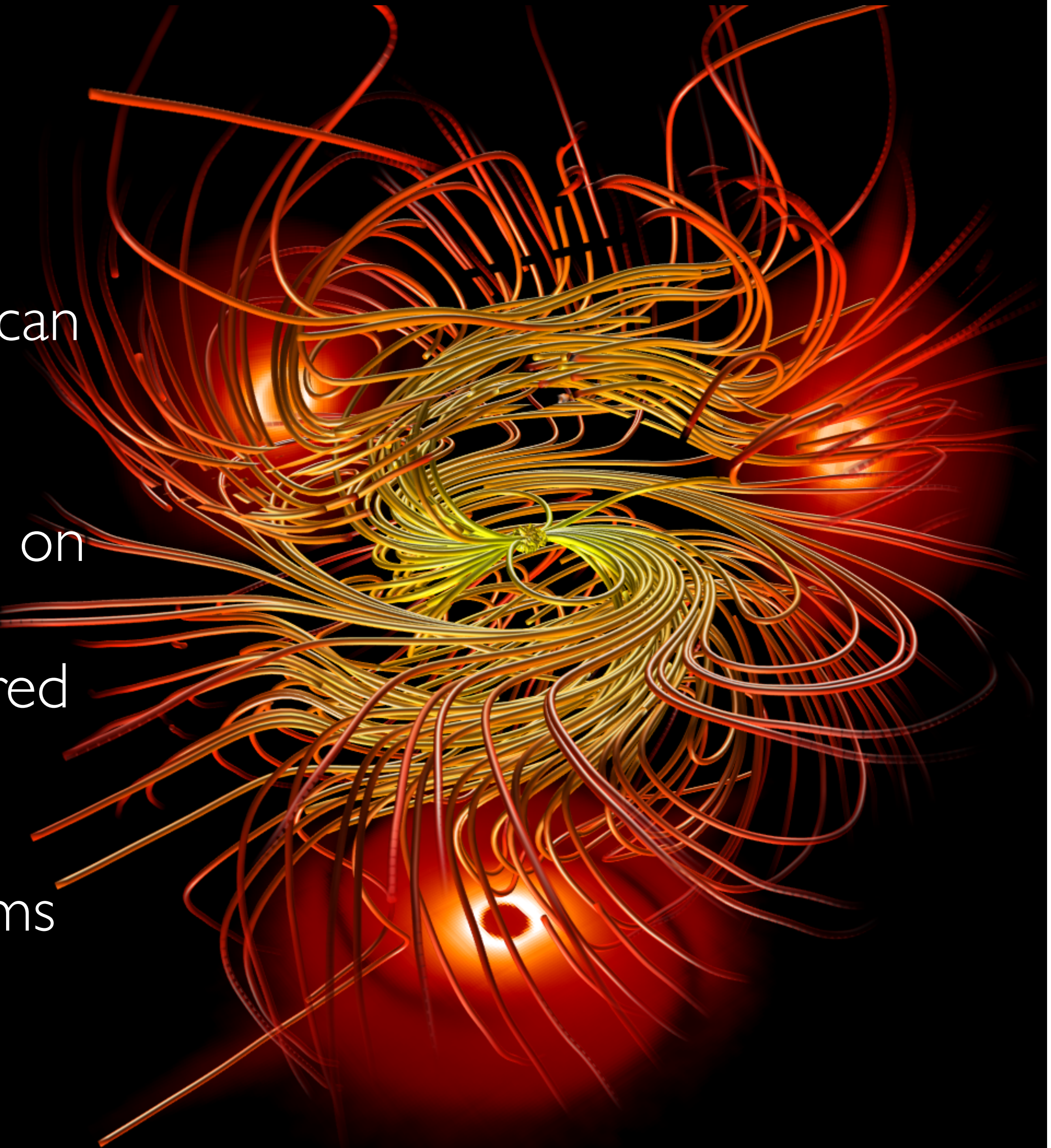

Outline

Particle in cell simulations towards the exascale

Laser particle acceleration and exotic beams

Exploring fundamental plasma processes for lab and astro

Moving to ultra high intensities

http://epp.ist.utl.pt/

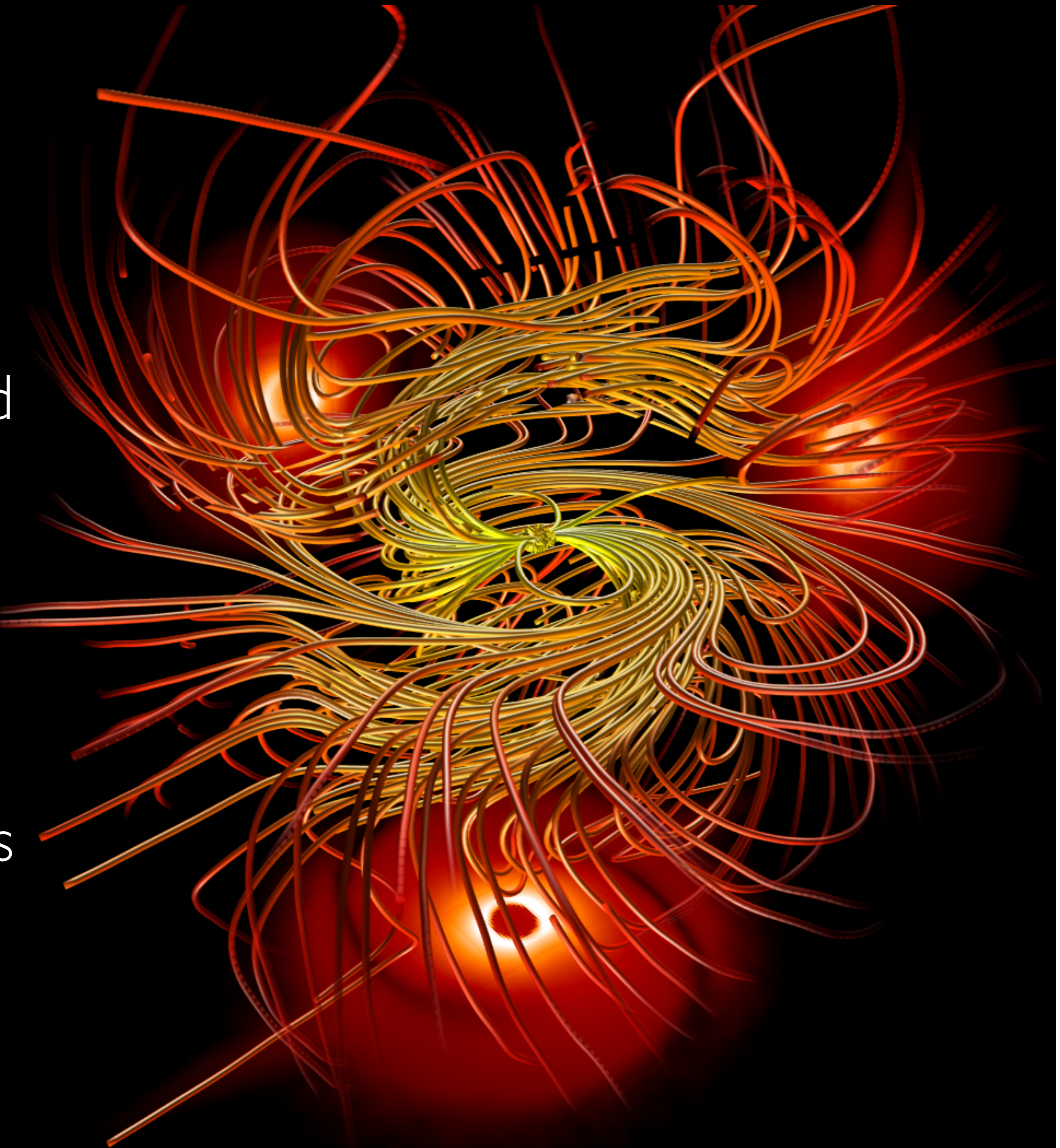

In the project Manhathan (c. 1940) the cost of one floating point operation was ~ 10^{-3}€

Operations performed in mechanical calculators.
Cost of labour ~ 4 €/hour, assuming one operation per second.
Total number of operation corresponding to 4 € = 1 flop/s 60 × 60 s

Today, in a graphics processor unit each floating point operation costs ~10^{-18} €

GPU performs 0.5 Tflop/s and costs ~ 2000 euros.
We assume a 3 year lifetime. Neglect the cost of electricity.
Total number of operation for 2000 euros = 0.5×10^{12} flop/s × 3 × 365 × 24 × 60 × 60 s

Particle-in-cell simulations

Solving Maxwell's equations on a grid with self-consistent charges and currents due to charged particle dynamics

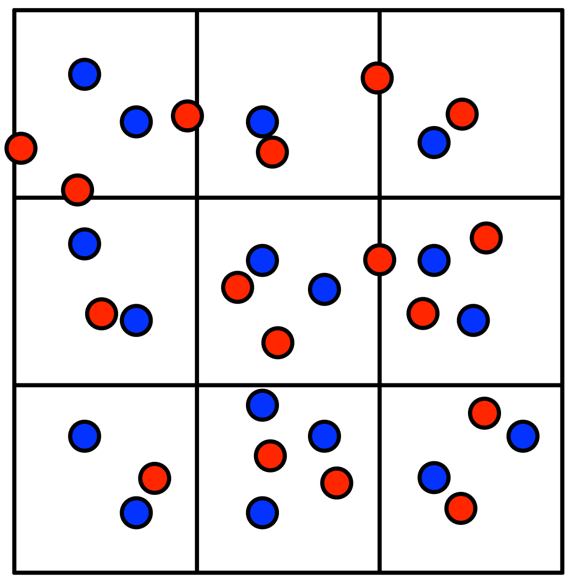

State-of-the-art

~ 10^{12} particles

~ $(12000)^3$ cells

RAM ~ 1 Gbyte - 100 TByte
Run time: hours to months
Data/run ~ few MB - 100s TByte

One-to-one simulations of plasma based accelerators & cluster dynamics
Weibel/two stream instability in astrophysics, relativistic shocks, fast igniton/inertial fusion energy, low temperature plasmas

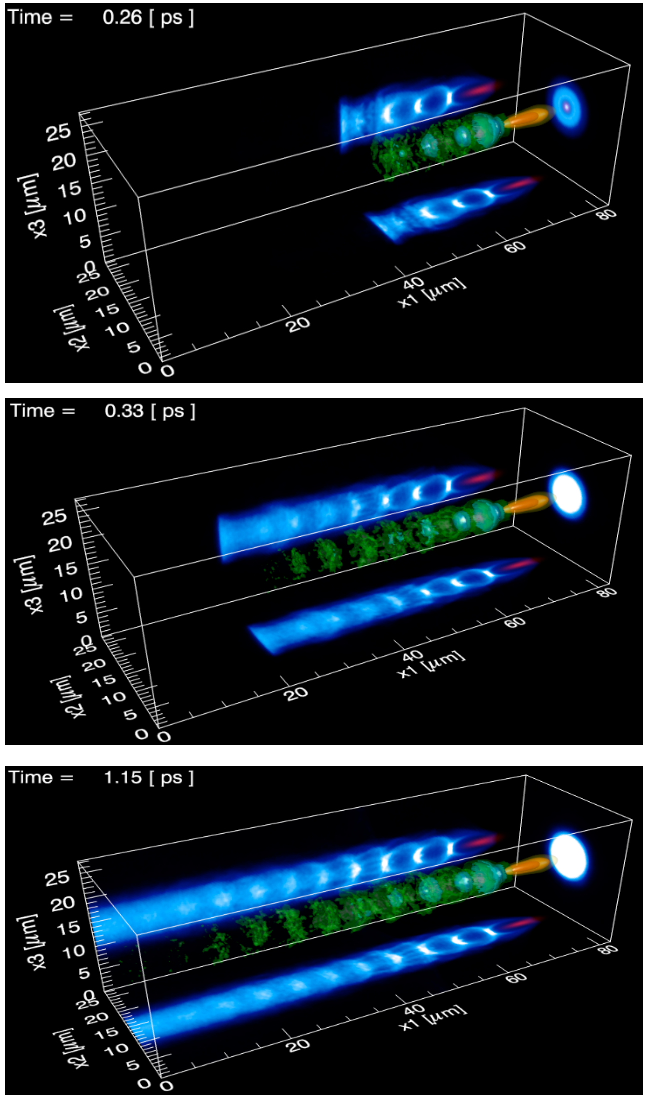

Particle-in-cell (PIC) - (Dawson, Buneman, 1960's)
Maxwell's equation solved on simulation grid
Particles pushed with Lorentz force

Osiris 3.0

osiris framework

- Massivelly Parallel, Fully Relativistic Particle-in-Cell (PIC) Code
- Visualization and Data Analysis Infrastructure
- Developed by the osiris.consortium
  ⇒ UCLA + IST

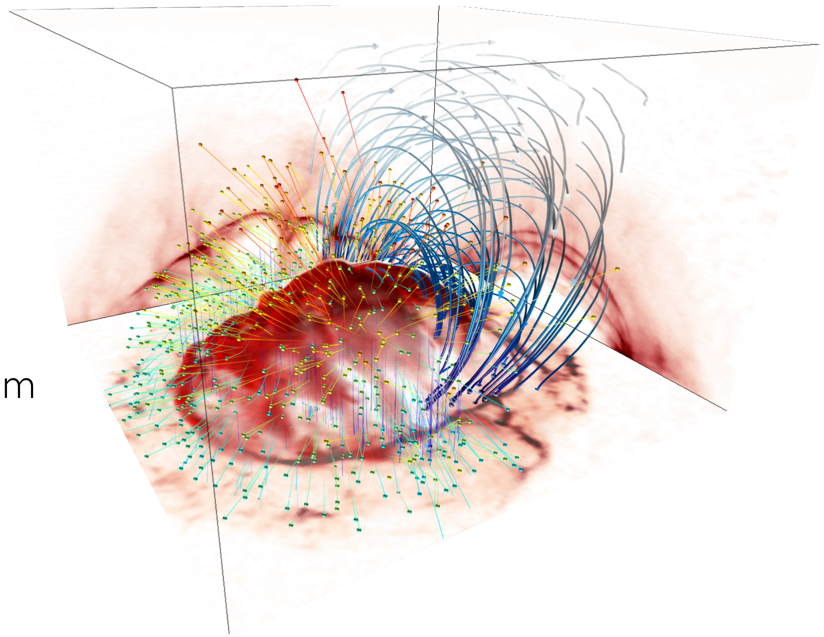

TÉCNICO LISBOA

UCLA

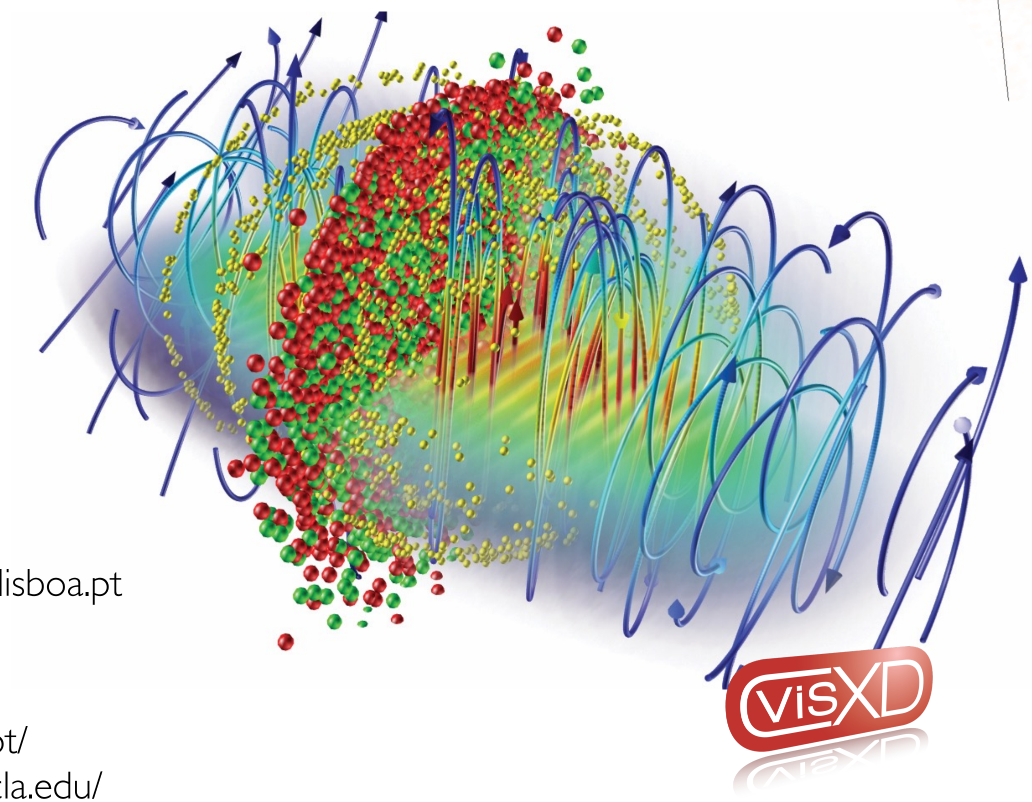

code features

- Scalability to ~ 1.6 M cores
- SIMD hardware optimized
- Parallel I/O
- Dynamic Load Balancing
- QED module
- Particle merging
- GPGPU support
- Xeon Phi support

Ricardo Fonseca
ricardo.fonseca@tecnico.ulisboa.pt
Frank Tsung
tsung@physics.ucla.edu

http://epp.tecnico.ulisboa.pt/
http://plasmasim.physics.ucla.edu/

QED-PIC loop + Particle Merging

osiris v2.0

INSTITUTO SUPERIOR TÉCNICO

UCLA

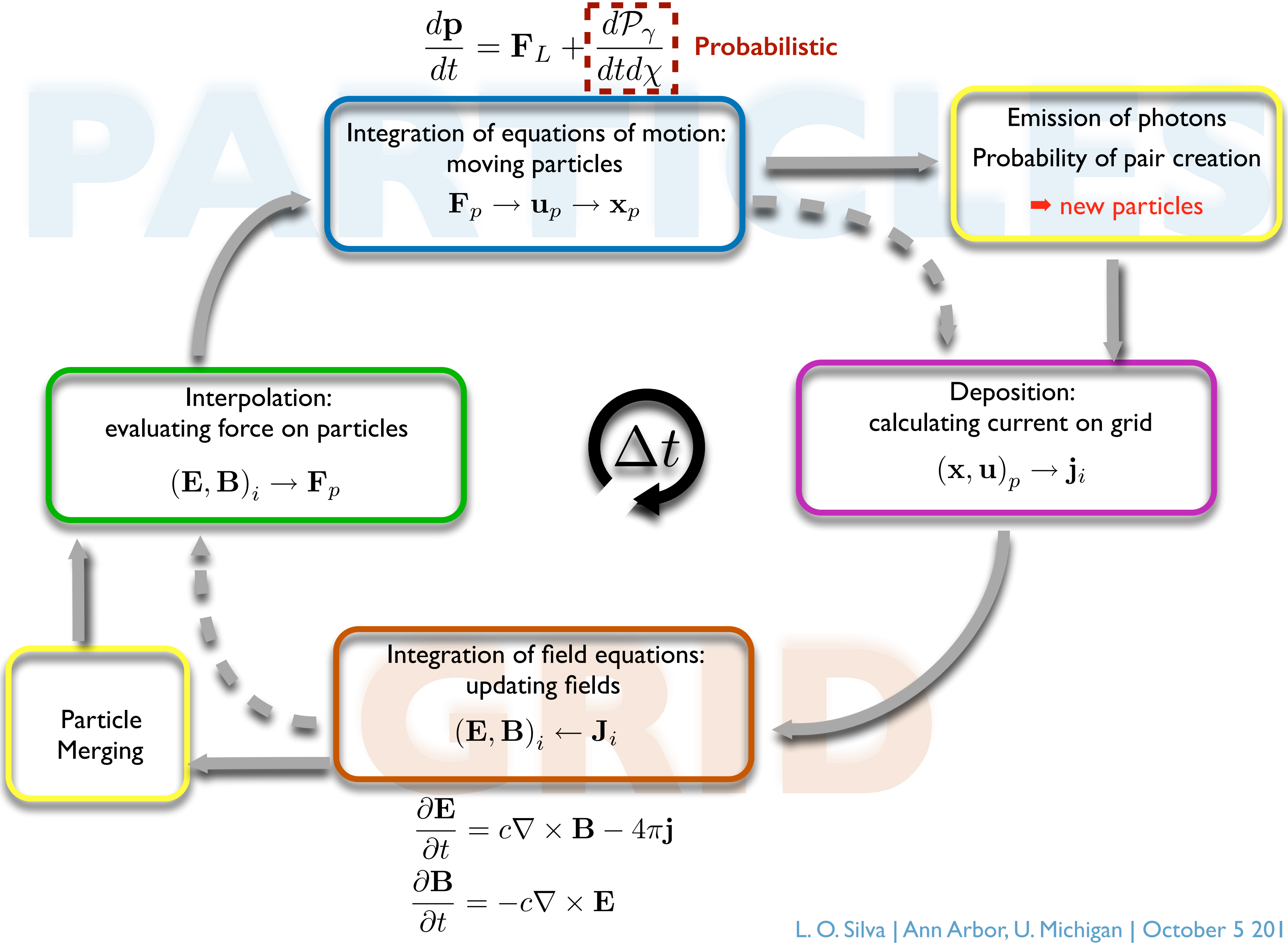

Extended to include QED effects

Emission Rate

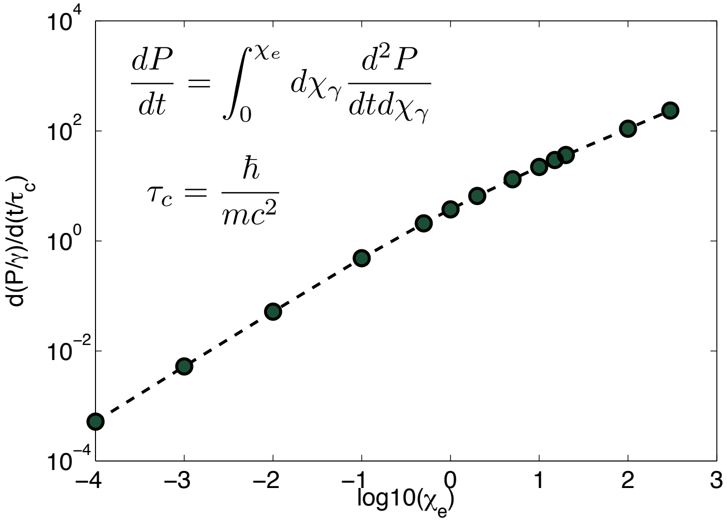

Pair creation rate

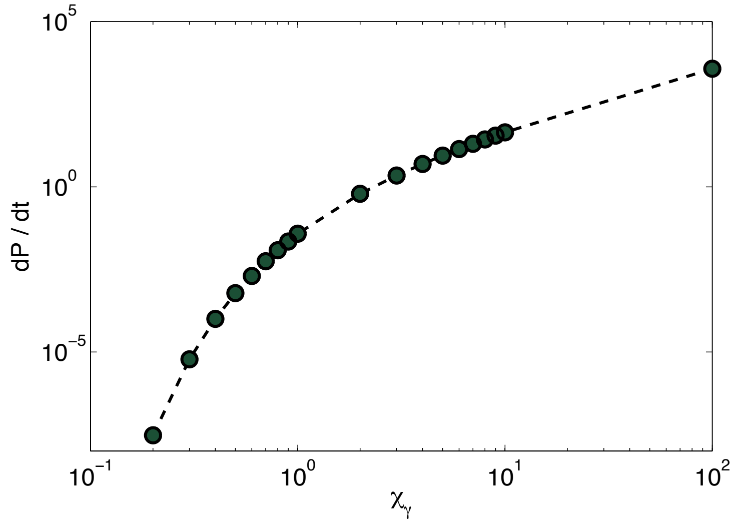

- **Additions to the PIC loop**
  - Quantum radiation reaction / photon emission
  - Photon propagation / Pair Creation
- **Study extreme lab / astrophysical scenarios**
  - Merge algorithm critical

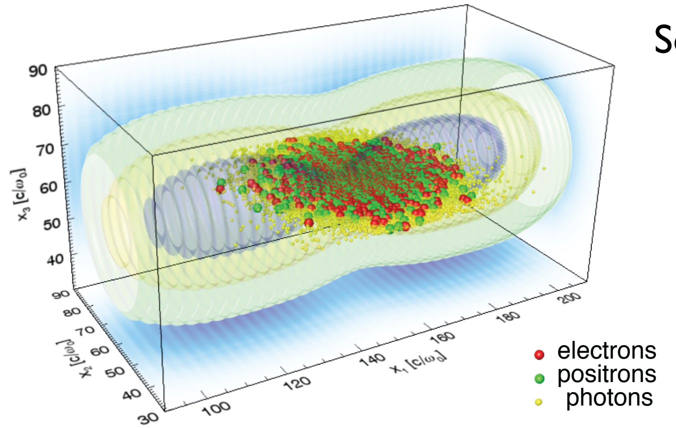

Seeded QED cascades in counter propagating laser pulses

Linear Polarization

T. Grismayer *et al.*, arXiv:1512.05174, PoP (2016)

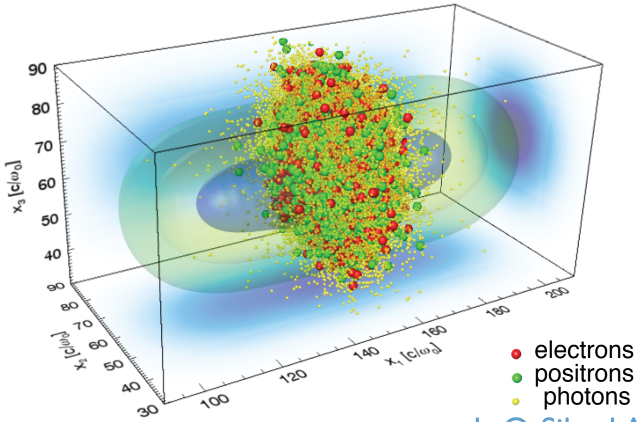

Double clockwise polarization

Merging algorithm addresses key challenge

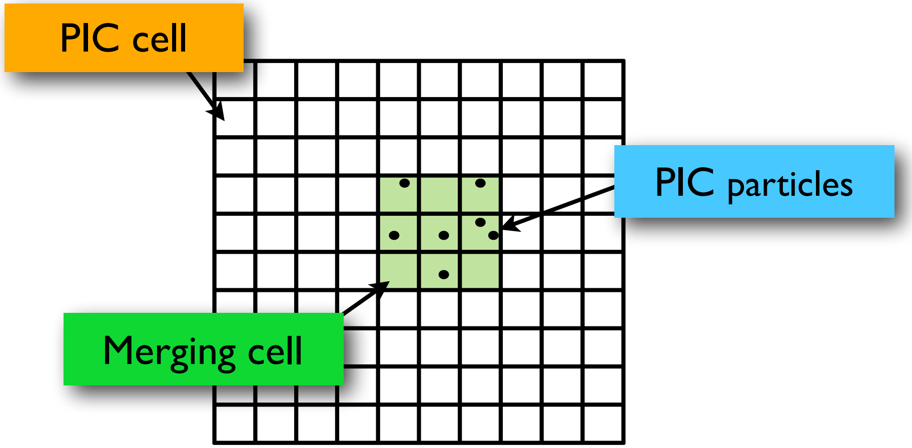

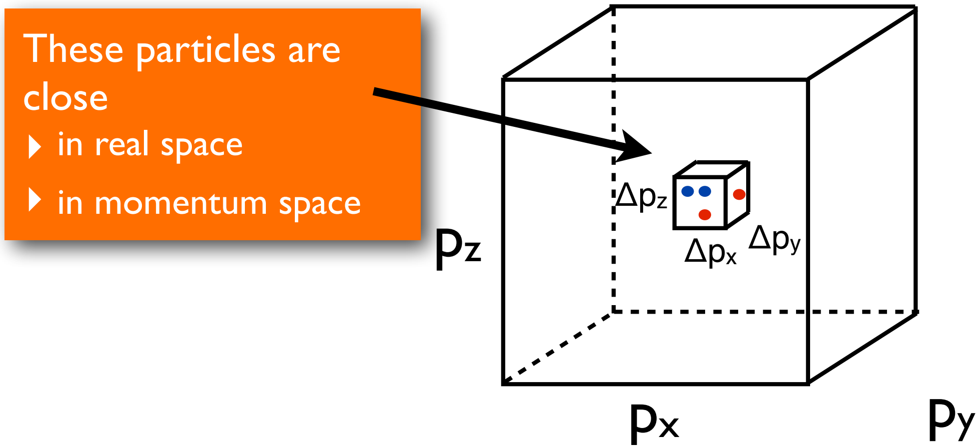

Equations to satisfy

$$w_t = w_a + w_b \ ,$$
$$\vec{p}_t = w_a \vec{p}_a + w_b \vec{p}_b$$
$$\epsilon_t = w_a \epsilon_a + w_b \epsilon_b$$

- **Dynamically resample the 6D phasespace**
  - Retain physical description of the system
  - Conserve charge, momentum and energy
- **Merge algorithm**
  - Find particles close enough in phasespace
  - Generate new particles observing conservation laws
- **Improve performance**
  - Fewer particles
  - Mitigate parallel load imbalance

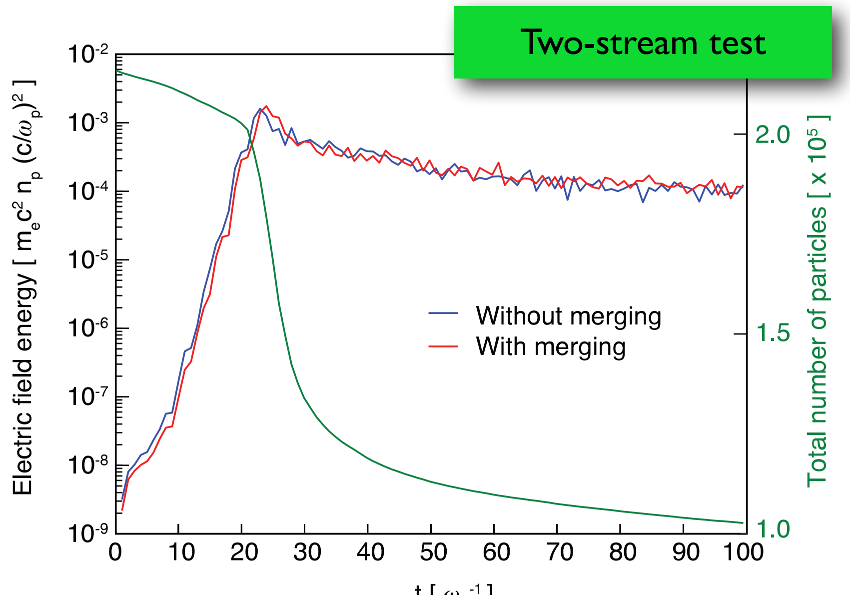

M. Vranic, *et al.*, Comput. Phys. Commun. **191**, 65-73 (2015)

Scaling Tests

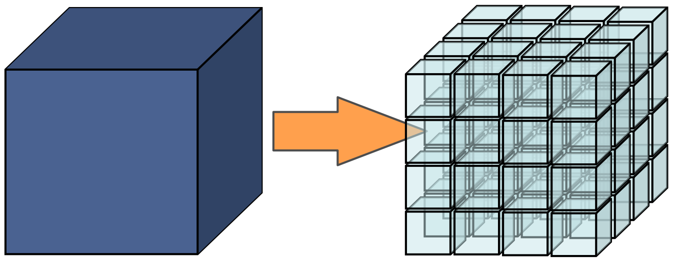

- Scaling tests on LLNL Sequoia
  4096 → 1572864 cores (full system)
- Warm plasma tests
  Quadratic interpolation
  $u_{th} = 0.1$ c
- Weak scaling
  Grow problem size
  cells = $256^3 \times (N_{cores} / 4096)$
  2^3 particles/cell
- Strong scaling
  Fixed problem size
  cells = 2048^3
  16 particles / cell

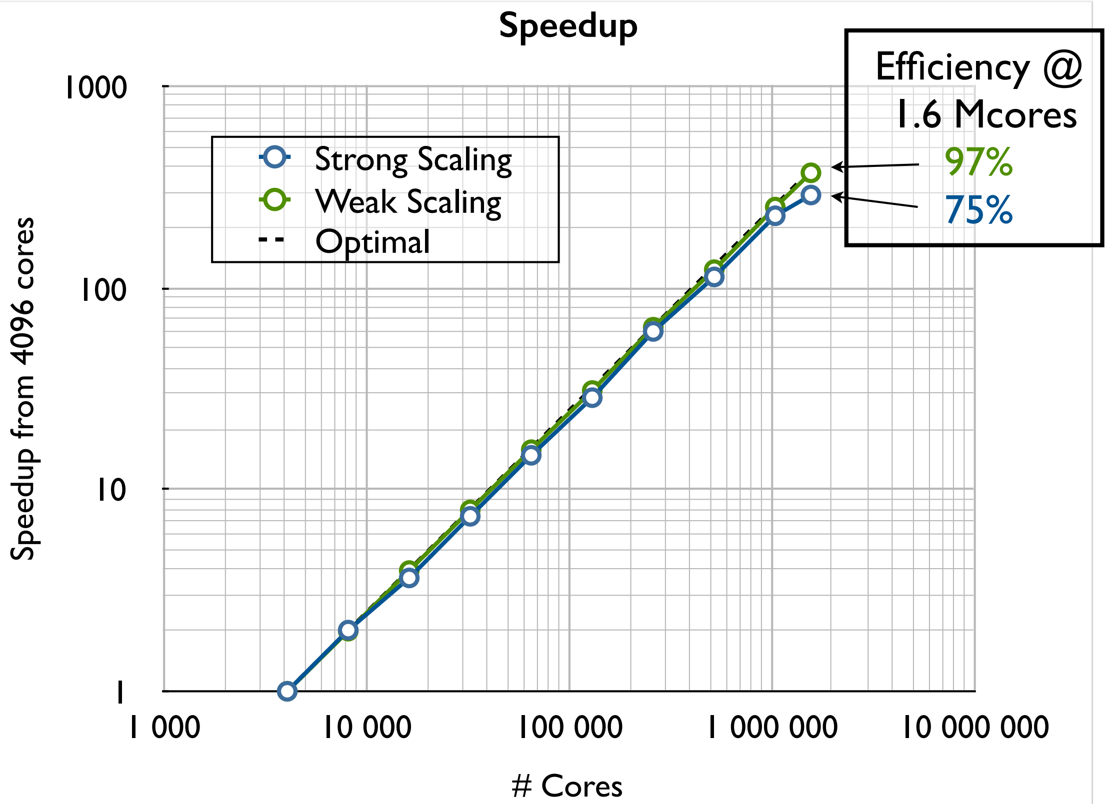

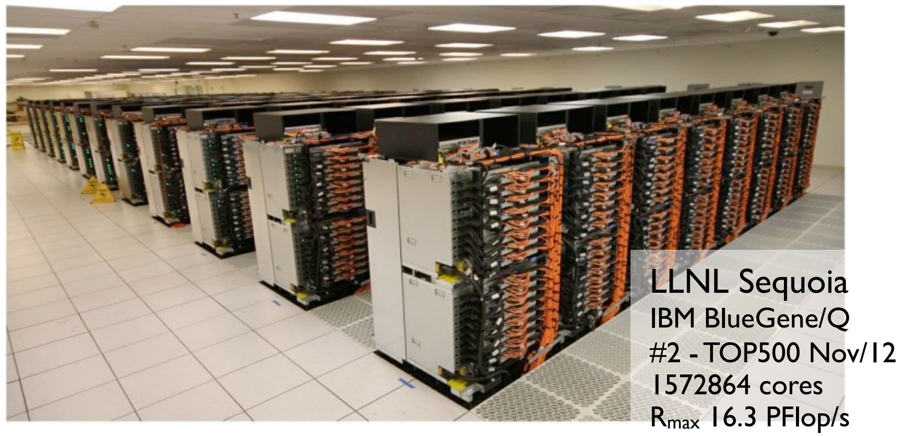

R. A. Fonseca *et al.* PPCF 55, 4011 (2013)

Similiar progress in supercomputers and intense lasers

Lasers and supercomputers

’14 Peak laser intensity ~ 10^{23} W/cm²

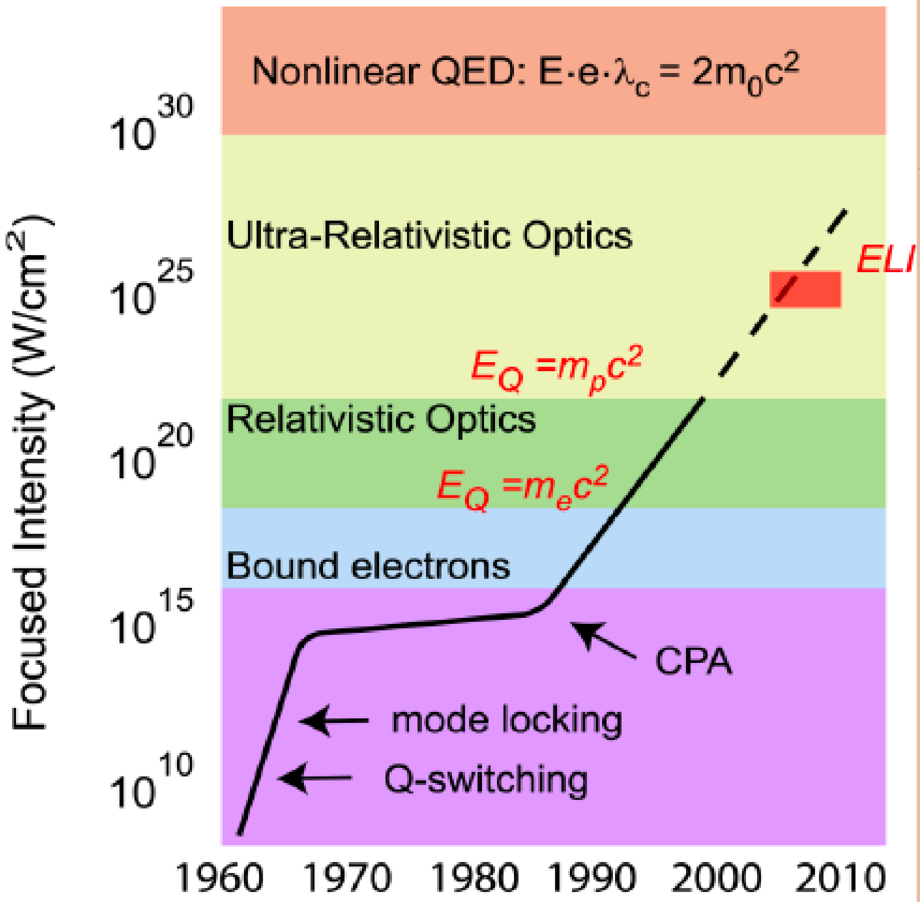

Mourou, Tajima, Bulanov (2006)

’14 Peak computing power > 10 Pflop/s

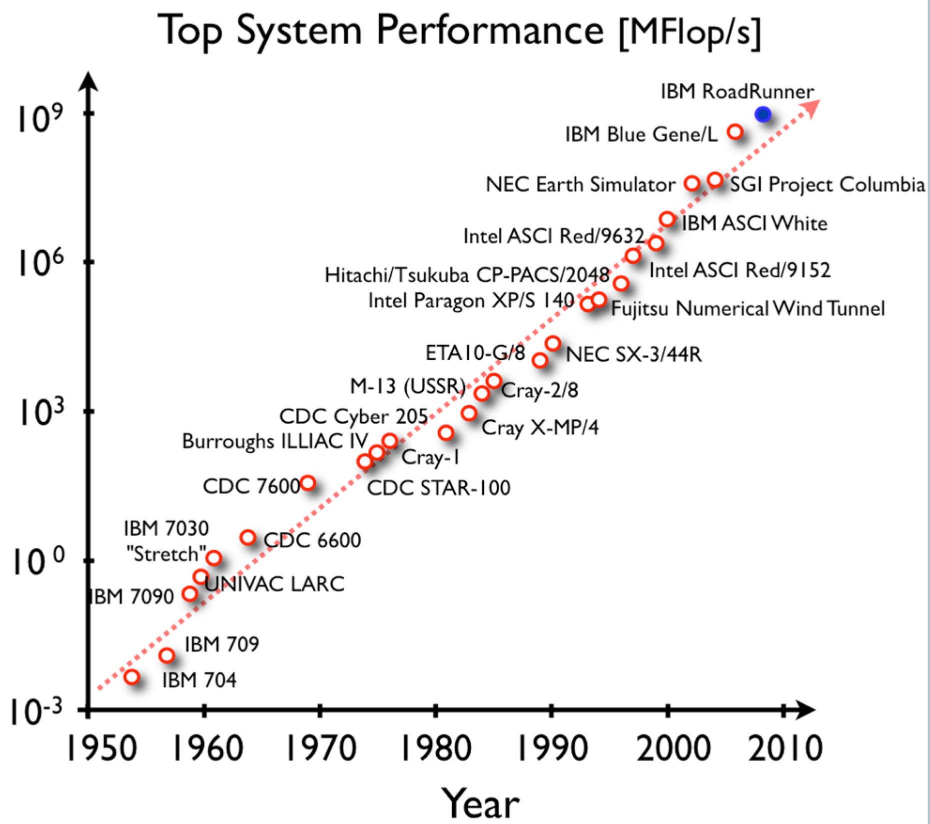

Source: top500.org

Similar intensities are present in particle beams

Existing or planned particle beams
LHC @ CERN I ~ 2.5×10^{19} W/cm^2 100 kJ, 7 TeV per proton, 10^{11} protons per beam; 10 cm long bunch; 200 microns spot
SPS @ CERN I ~ 1.5×10^{18} W/cm^2 ~7 kJ, 0.5 TeV per proton, 10^11 protons per beam; 10 cm long bunch; 200 microns spot
ILC I ~ 1.5×10^{24} W/cm^2 1.6 kJ, 0.5 TeV per electron/positron, 2×10^{10} electrons/positrons; < 10 nm width in x; < ~100 nm width in y; 6 mm long
SLAC I ~ 1.2×10^{19} W/cm^2 160 J, 50 GeV per electron/positron, 2×10^{10} electrons/positrons; ~50 microns long; ~50 microns spot

Outline

Particle in cell simulations towards the exascale

Laser particle acceleration and exotic beams

Exploring fundamental plasma processes for lab and astro

Moving to ultra high intensities

http://epp.ist.utl.pt/

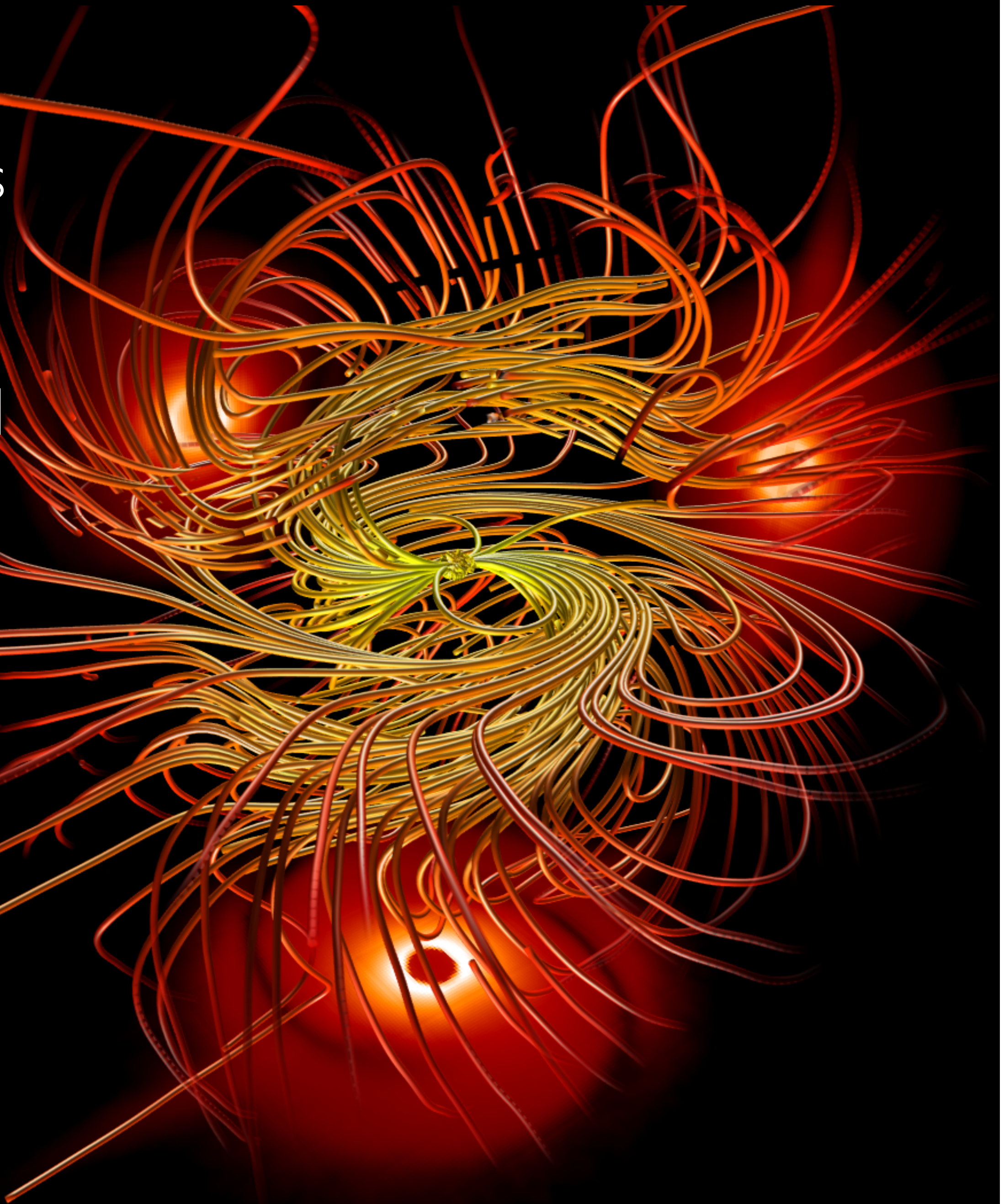

Next generation of lasers @ 10+ PW

central laser facility

Science & Technology Facilities Council

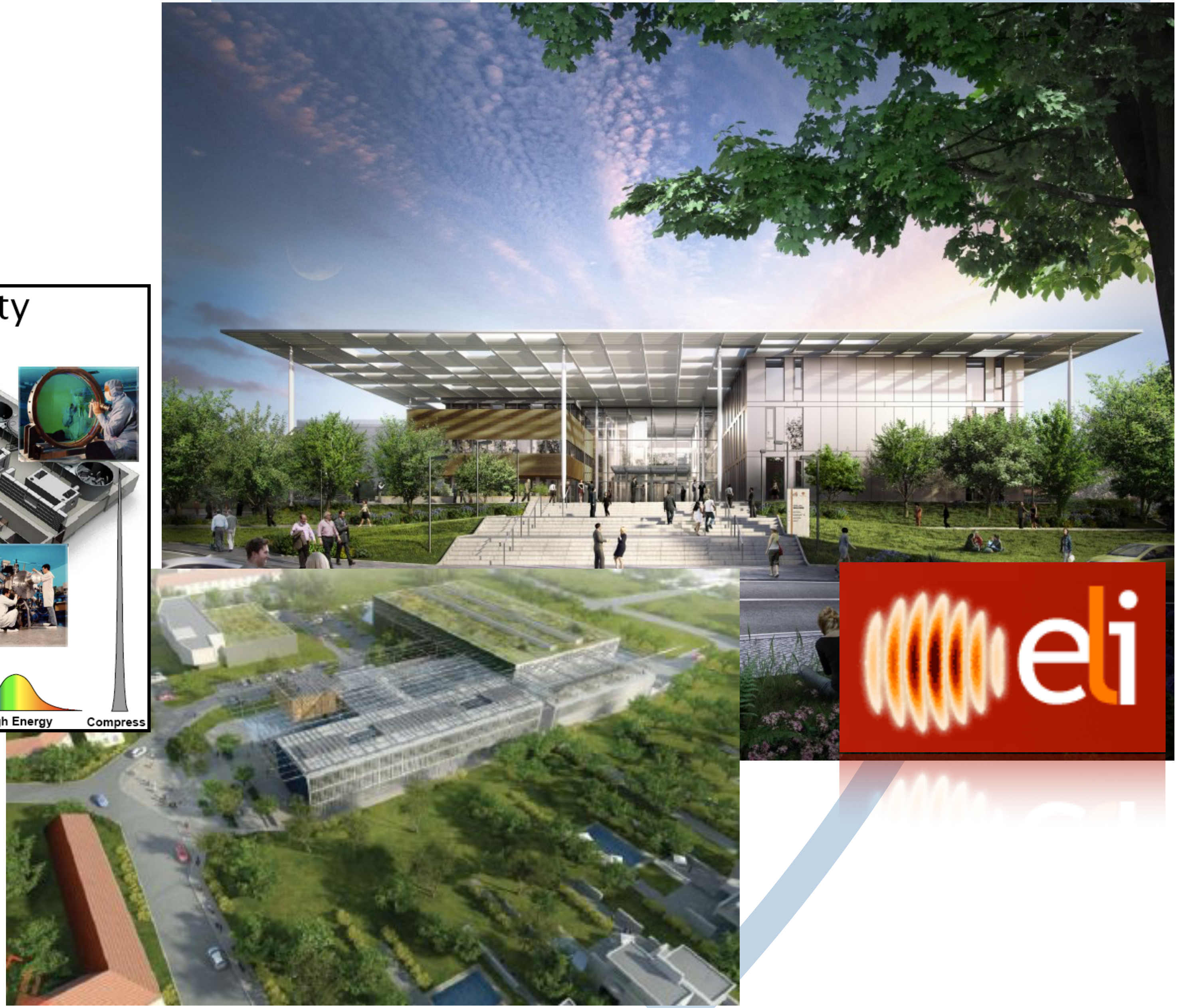

eli

Blow-out regime of laser wakefield acceleration

Self-injection, Dephasing, and Depletion

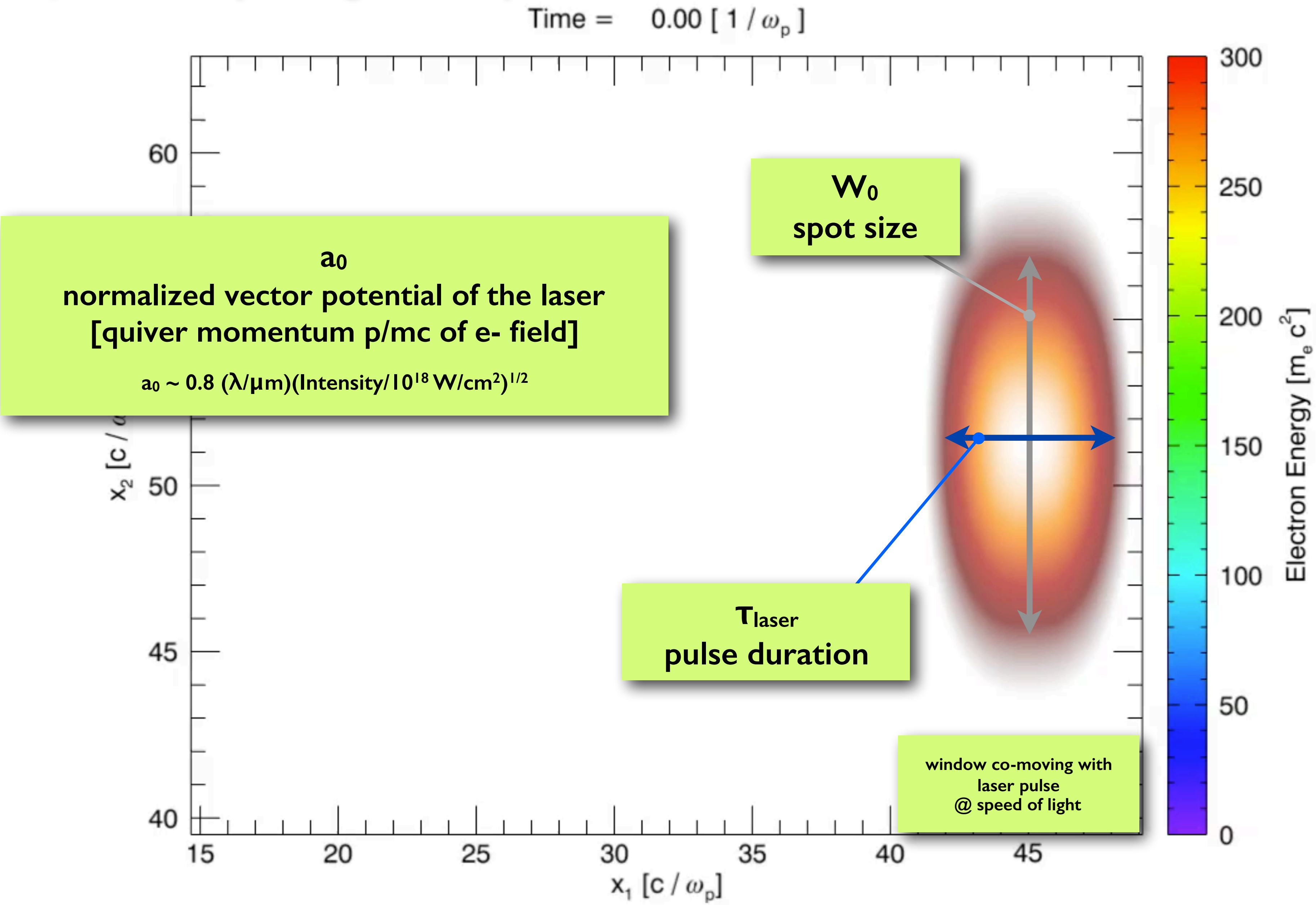

Energy frontier LWFA @ 250 J

Extreme blowout :: a_0=53

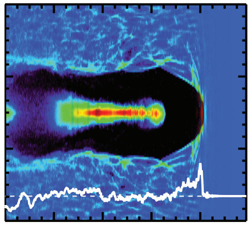

- Very nonlinear and complex physics
- Bubble radius varies with laser propagation
- Electron injection is continuous ⇒ very strong beam loading
- Wakefield is noisy and the bubble sheath is not well defined

few GeV

Controlled self-guided :: a_0=5.8

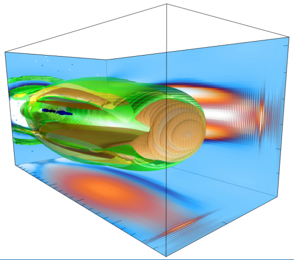

- Lower laser intensity ⇒ cleaner wakefield and sheath
- Loaded wakefield is relatively flat
- Blowout radius remains nearly constant
- Three distinct bunches ⇒ room for tuning the laser parameters

~10-15 GeV

Channel guided :: a_0=2

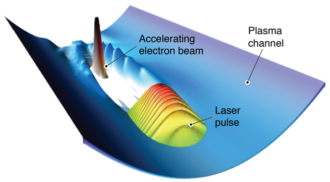

- Lowest laser intensity ⇒ highest beam energies (less charge)
- External guiding of the laser ⇒ stable wakefield
- Tailored electron beam that initially flattens the wake
- Controlled acceleration of an externally injected beam to very high energies

~30-40 GeV

S. Gordienko and A. Pukhov PoP (2005); W. Lu et al. PR-STAB (2007)
S. F. Martins et al., Nature Physics (2009)

The orbital angular momentum of light is an unexplored degree of freedom for laser-plasma interactions

Production/ amplification of OAM lasers via Stimulated Raman Amplification: J.Vieira *et al.*, Nat. Comms (2016)

Helical wavefronts

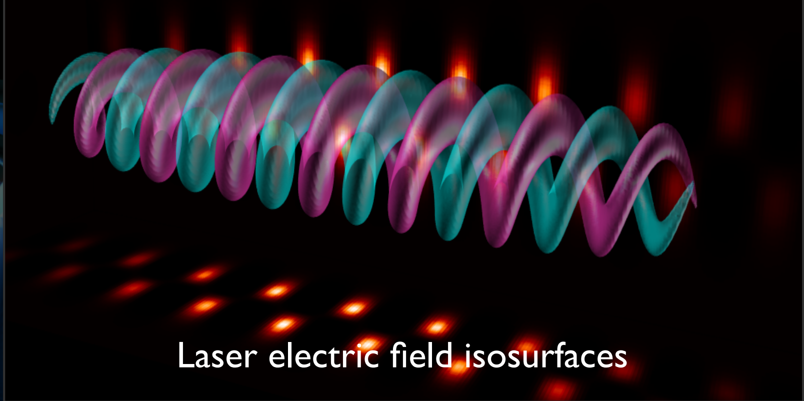

Laser electric field isosurfaces

Donut-shaped intensity profiles

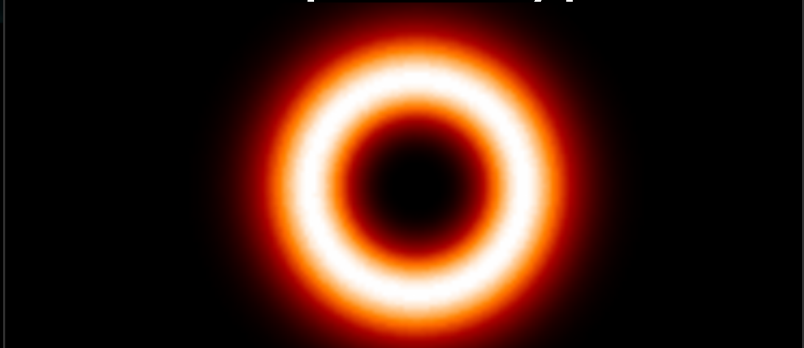

Transverse slice of laser envelope

Applications

- Astrophysics
- Ultrafast optical communications
- Nano particle manipulation

Laser-plasma accelerators

Shaped electron/x-ray beams

Ion acceleration (maybe reduce divergence)

High gradient positron acceleration

Laguerre-Gaussian lasers drive exotic (e.g. doughnut like) plasma waves in strongly non-linear regimes

Linear doughnut wakefields

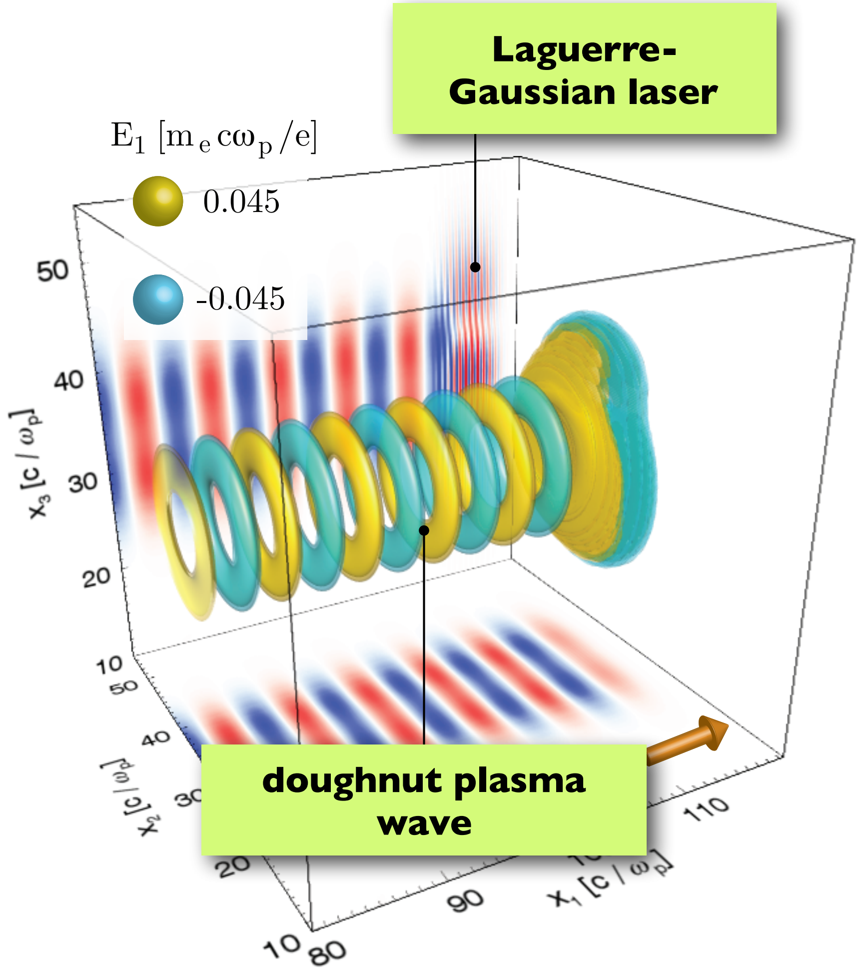

J.T. Mendonça and J.Vieira, PoP **21**, 033107 (2014)

Non-linear doughnut bubbles

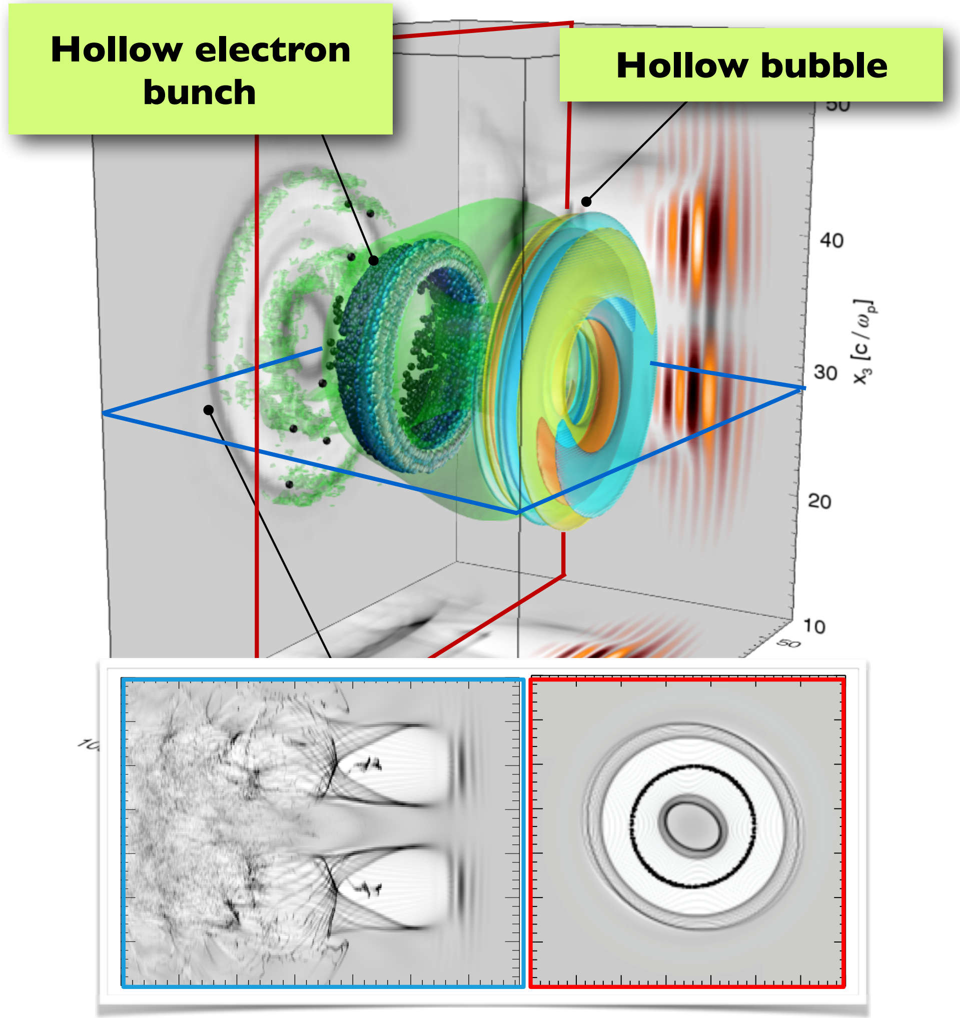

J.Vieira and J.T. Mendonça PRL **112**, 215001 (2014)

e-e+ fireballs from laser generated beams in solids

Experimental results demonstrate formation of e-e+ fireball

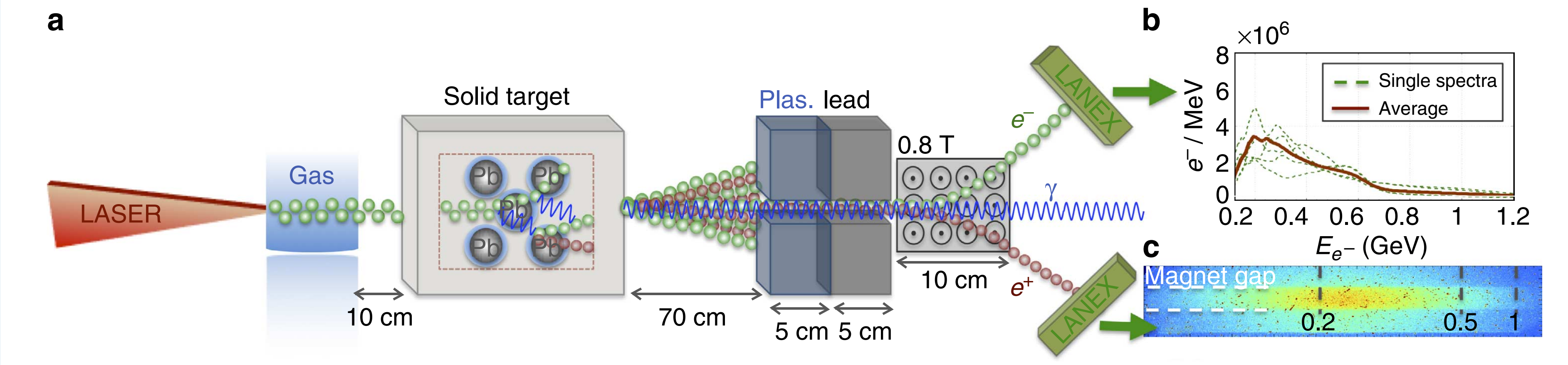

e-e+ fireball is neutral

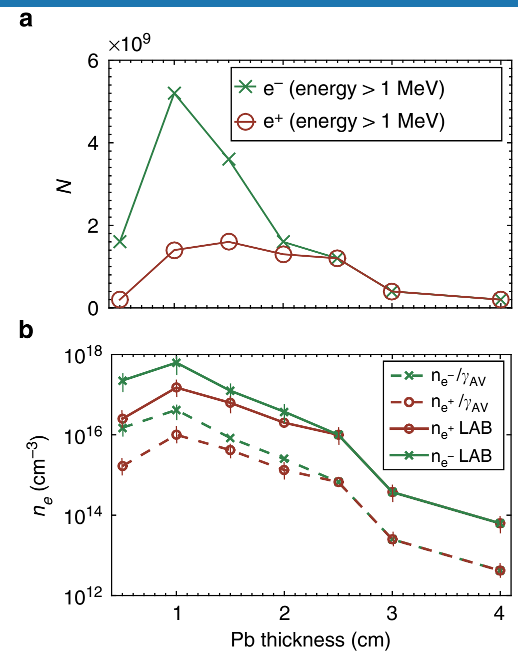

G. Sarri *et al.*, Nature Communications (2015)

e-e+ fireballs to explore Weibel instability

LWFA fireball beam will undergo current filamentation instability

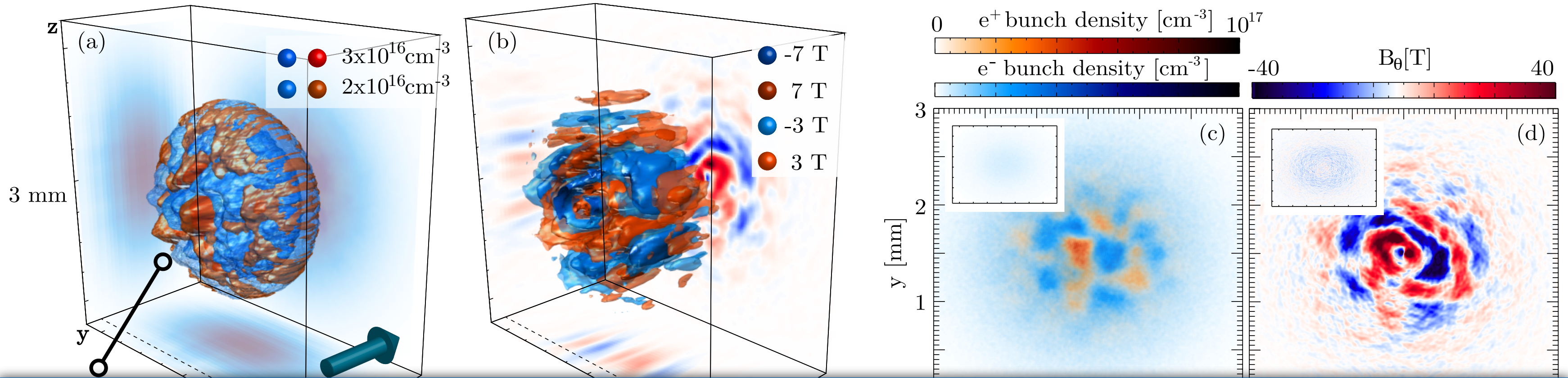

G. Sa

e-e+ plasma

Additional source of secondary radiation (e.g. gamma rays)

Platform to understand microinstabilities of relevance in astrophysics

"Dark electromagnetism"

29

$\sigma_x = \sigma_y = 2\sigma_z = 20\ \mu m$

$\text{Emittance} = 10^{-5}\ \text{mrad}$

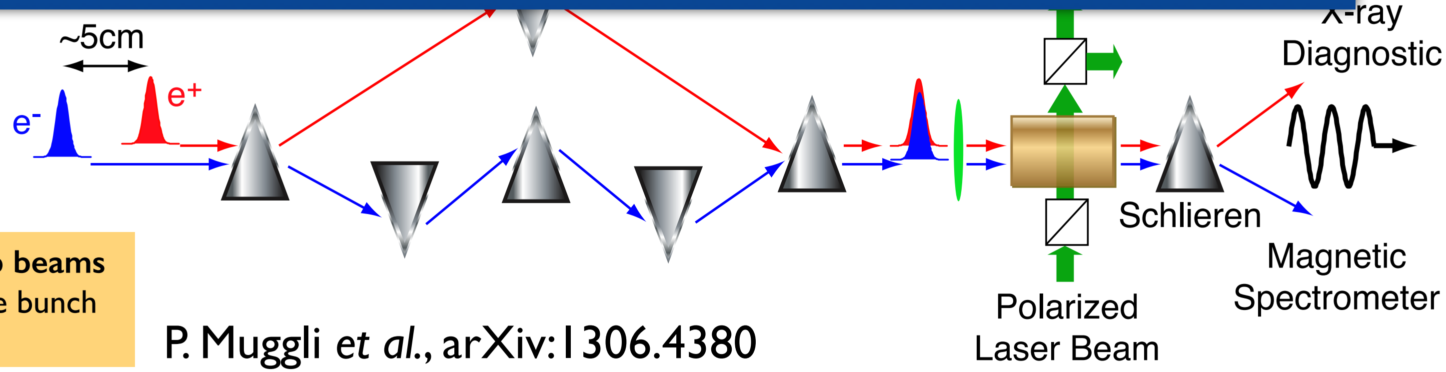

Dephasing technique to overlap beams

Typically used in PWFA to reduce bunch distance to ~100 microns

P. Muggli *et al.*, arXiv:1306.4380

Interaction of fireball beam with plasma generates current filamentation instability (CFI)

Beam density

Filament size ~ 0.5 λ_{pe}

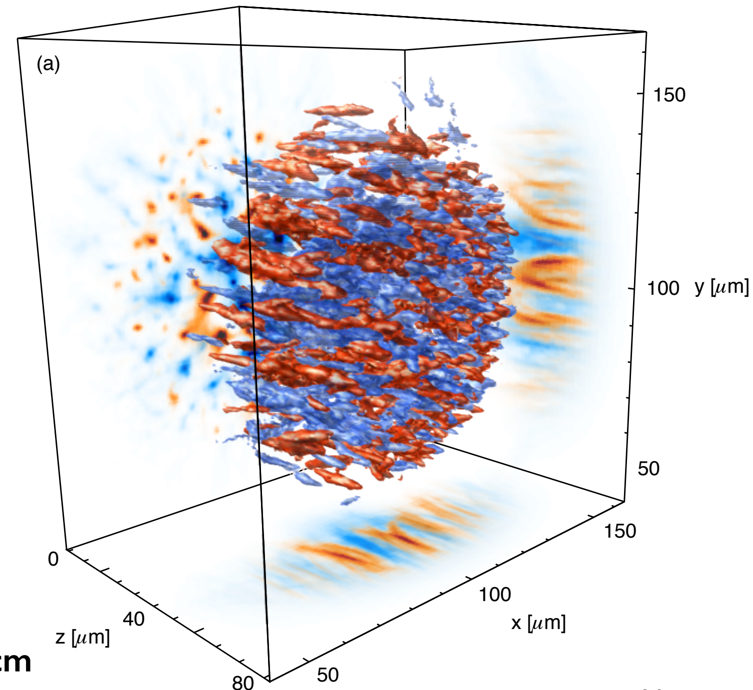

Distance : 1.5 cm

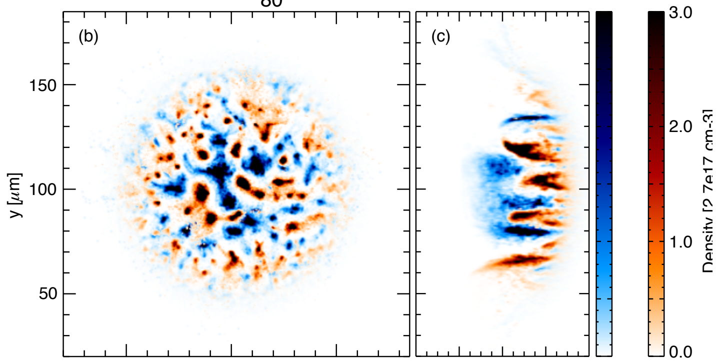

Growth of B3-field

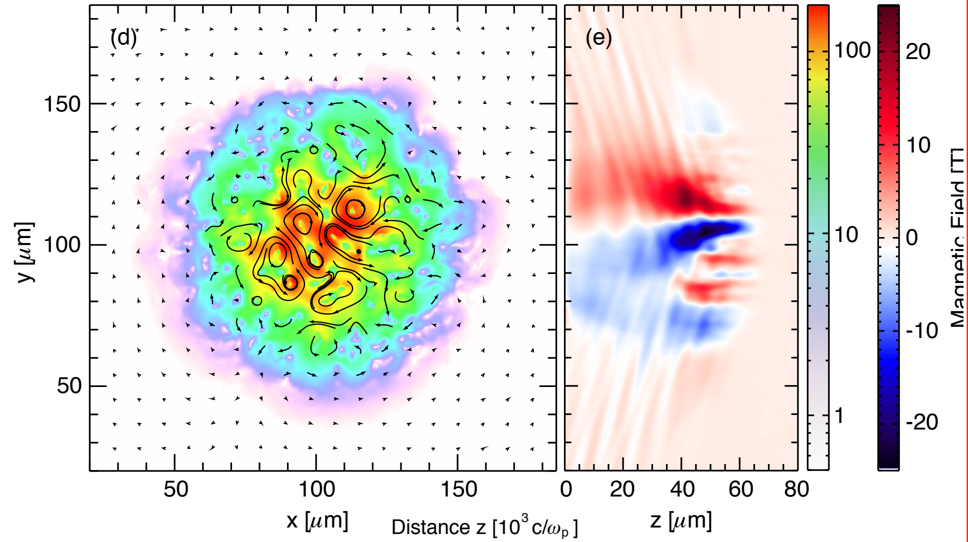

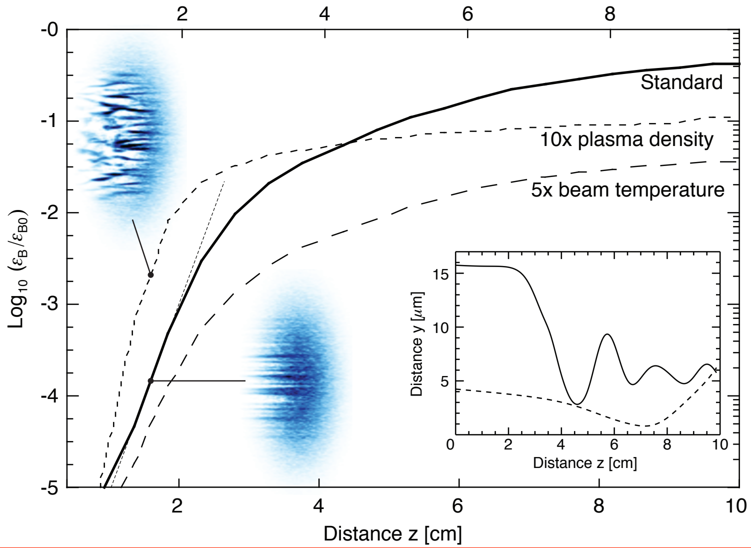

Onset of CFI is determined by the balance between the beam emittance and CFI growth rate

- Rate of beam expansion can be expressed by the envelope equation as the function of beam emittance

$$\boxed{\frac{1}{\sigma_b}\frac{\mathrm{d}\sigma_b}{\mathrm{dt}} = \frac{t\ c^2\ \epsilon_N^2}{\sigma_{b0}^2\gamma_b^2} \ll \boxed{\frac{\omega_{pe}}{\sqrt{\gamma_b}}}}$$

Growth of CFI

where σ_b is the beam radius, γ_b is relativistic factor and ϵ_N (=$p_r\ \gamma_b$) is normalised beam emittance

- The criteria for CFI growth is that the beam expansion rate is much smaller than the CFI growth rate

$$\boxed{\theta \ll \left(\frac{\Gamma_{CFI}\sigma_{b0}^2}{L_{growth}c}\right)^{1/2}}$$

where $\theta = \langle p_\perp \rangle / \gamma_b$ and we have considered that t ~L_{growth}/c, L_{growth} is the growth length of CFI.

Transition from CFI to Oblique instability

- **Going from short beam to longer beam**

  Density ratio is decreased i.e. for longer beam the plasma is overdense $\omega_{pe} \gg \omega_{be}$

  The growth rate of the two-streaming instability can be significant

Growth rate of Oblique and CFI

$$\Gamma_{OBI} \simeq \frac{\sqrt{(3)}}{2^{4/3}} \frac{\alpha^{1/3}}{\gamma_{b0}} \;\; ; \;\; \Gamma_{CFI} \simeq \sqrt{\frac{\alpha}{\gamma_{b0}}}$$

$$\frac{\Gamma_{OBI}}{\Gamma_{CFI}} = \frac{\sqrt{3}}{2^{4/3}} \frac{1}{\beta_b} \left(\frac{\gamma_b}{\alpha}\right)^{1/6}$$

where $\alpha = n_{b0}/n_{p0}$

Far smaller density ratio, oblique instability may be greater or comparable to the CFI

Three dimensional simulations confirm the growth of the OBI for smaller density ratios

Signature of Oblique mode

Drives wakefield structure

Tilting of B-field lines

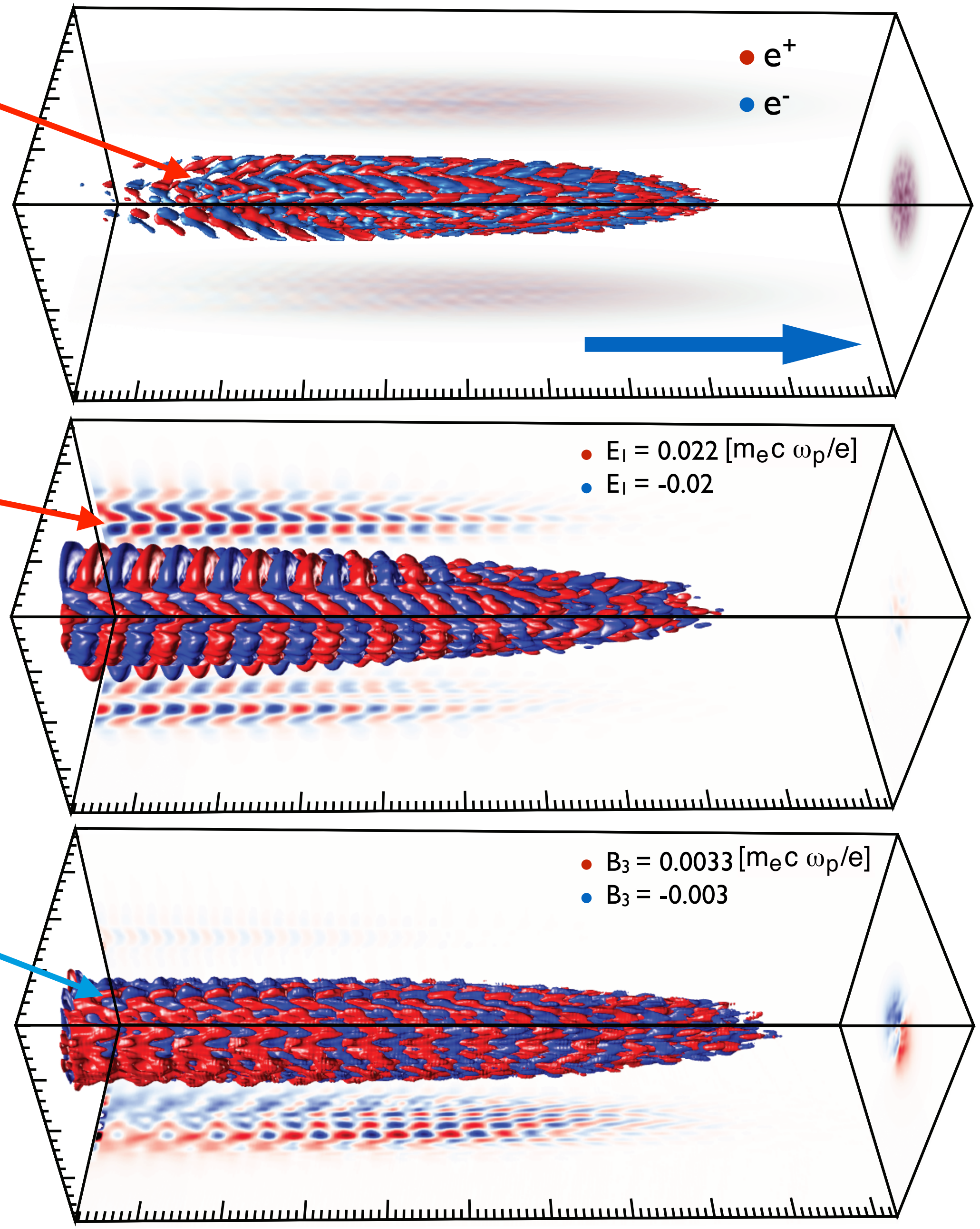

Outline

Particle in cell simulations towards the exascale

Laser particle acceleration and exotic beams

Exploring fundamental plasma processes for lab and astro

Moving to ultra high intensities

http://epp.ist.utl.pt/

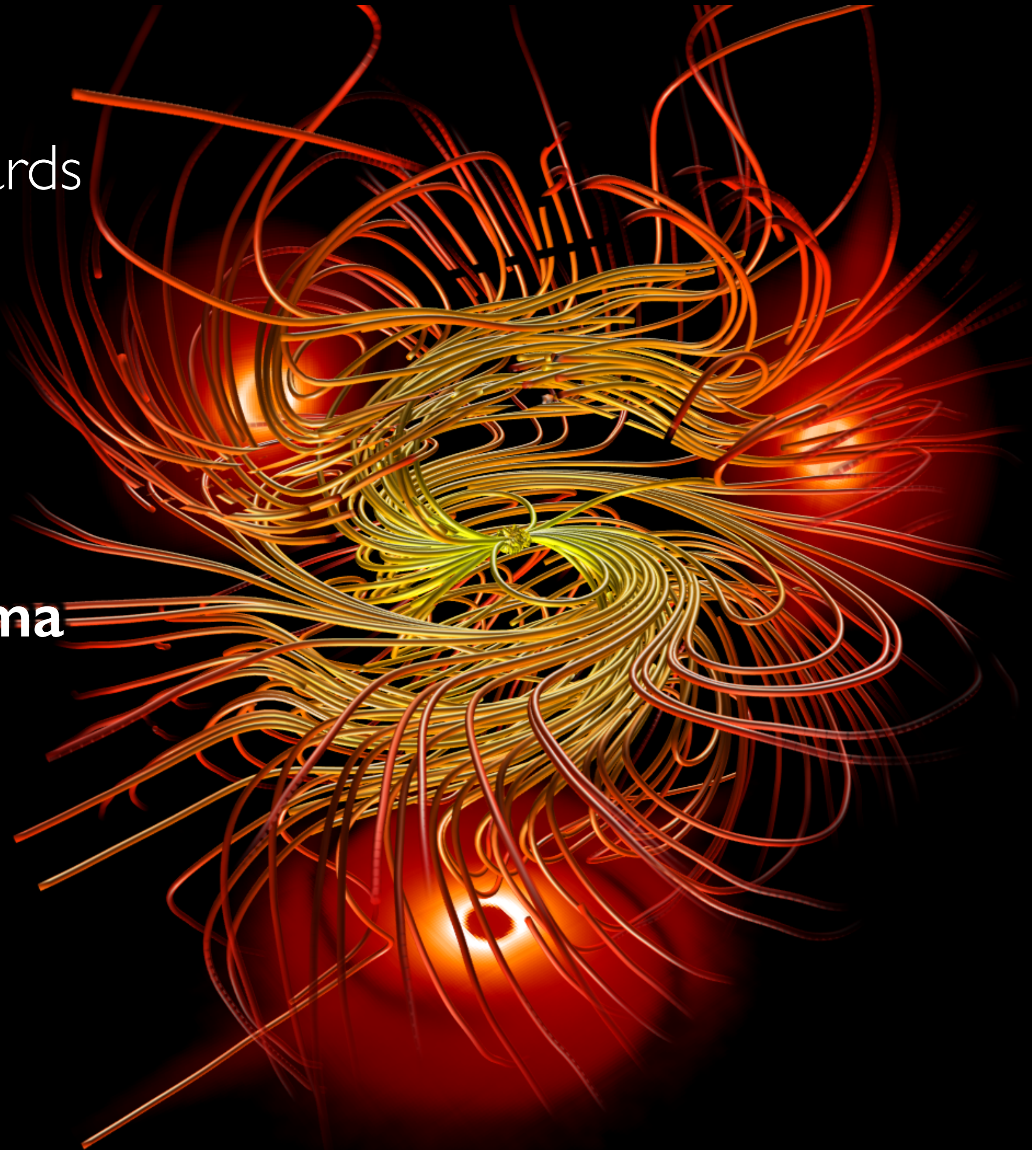

Plasma instabilities critical to shock formation and field structure

- **B-fields generated by current filamentation/Weibel in GRBs**
  [Medvedev & Loeb, Gruzinov & Waxman, 99, Silva et al, 03]

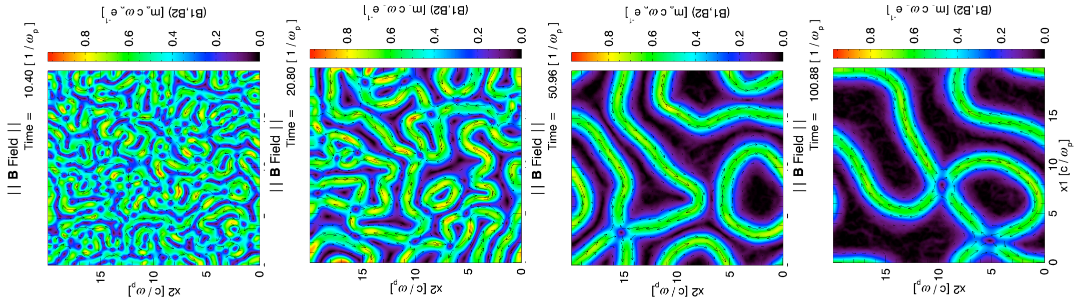

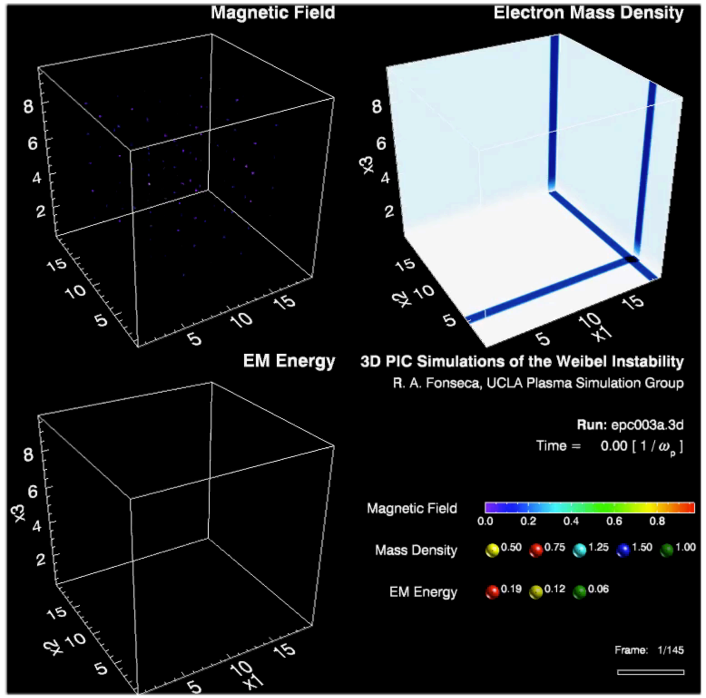

- **Fields in relativistic shocks** are mediated by Weibel/current filamentation generated fields
  [Spiktovsky 08, Martins et al., 09]

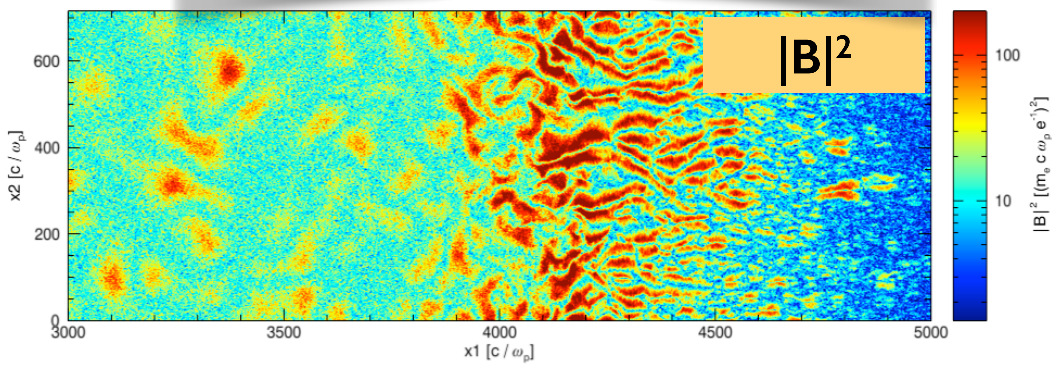

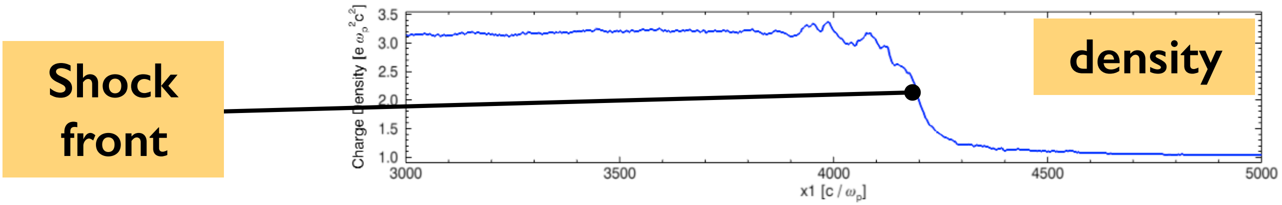

Collision of two relativistic plasma slabs

Simulation apparatus

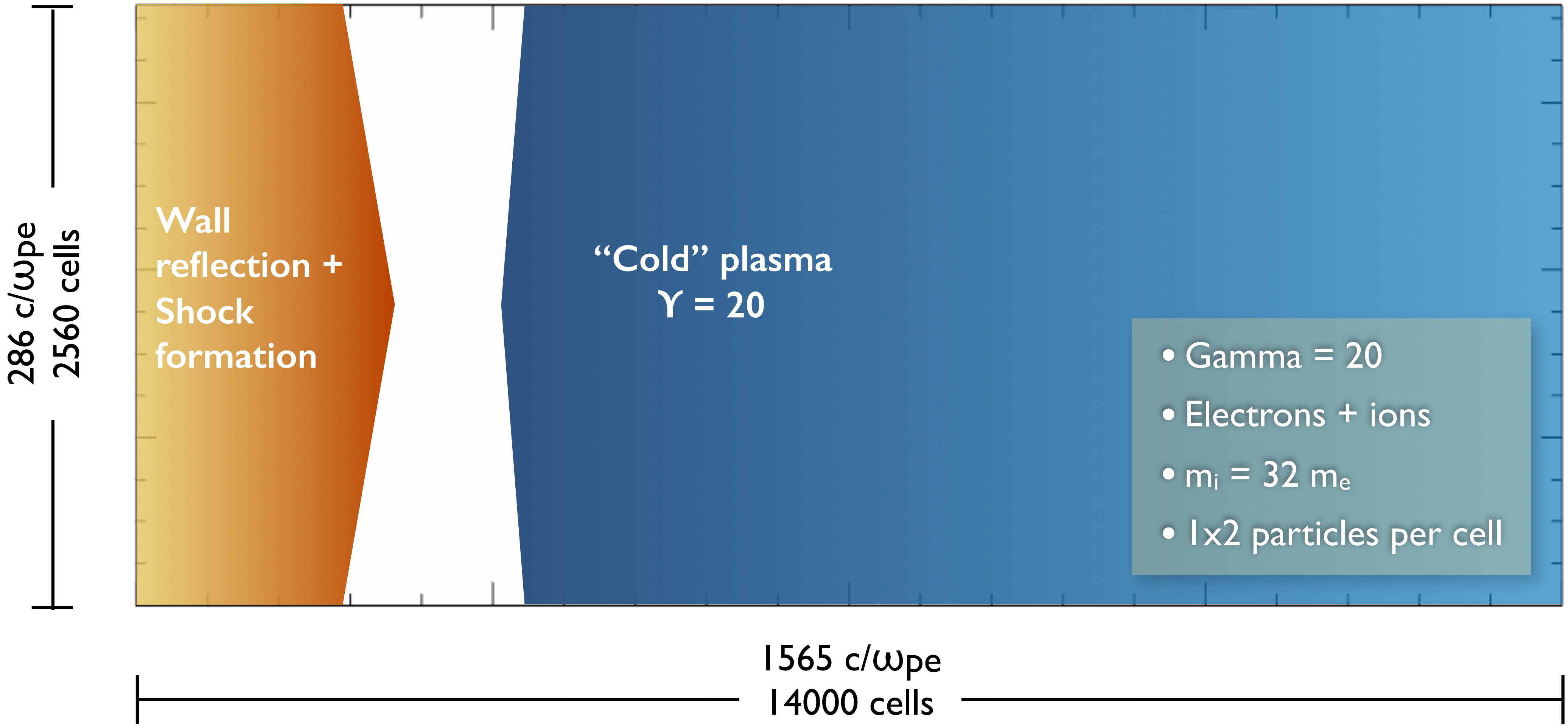

A. Spitkovsky, ApJ Lett (2008)
S. F. Martins *et al.*, ApJ Lett (2009)

Shock formation and evolution

Ion density

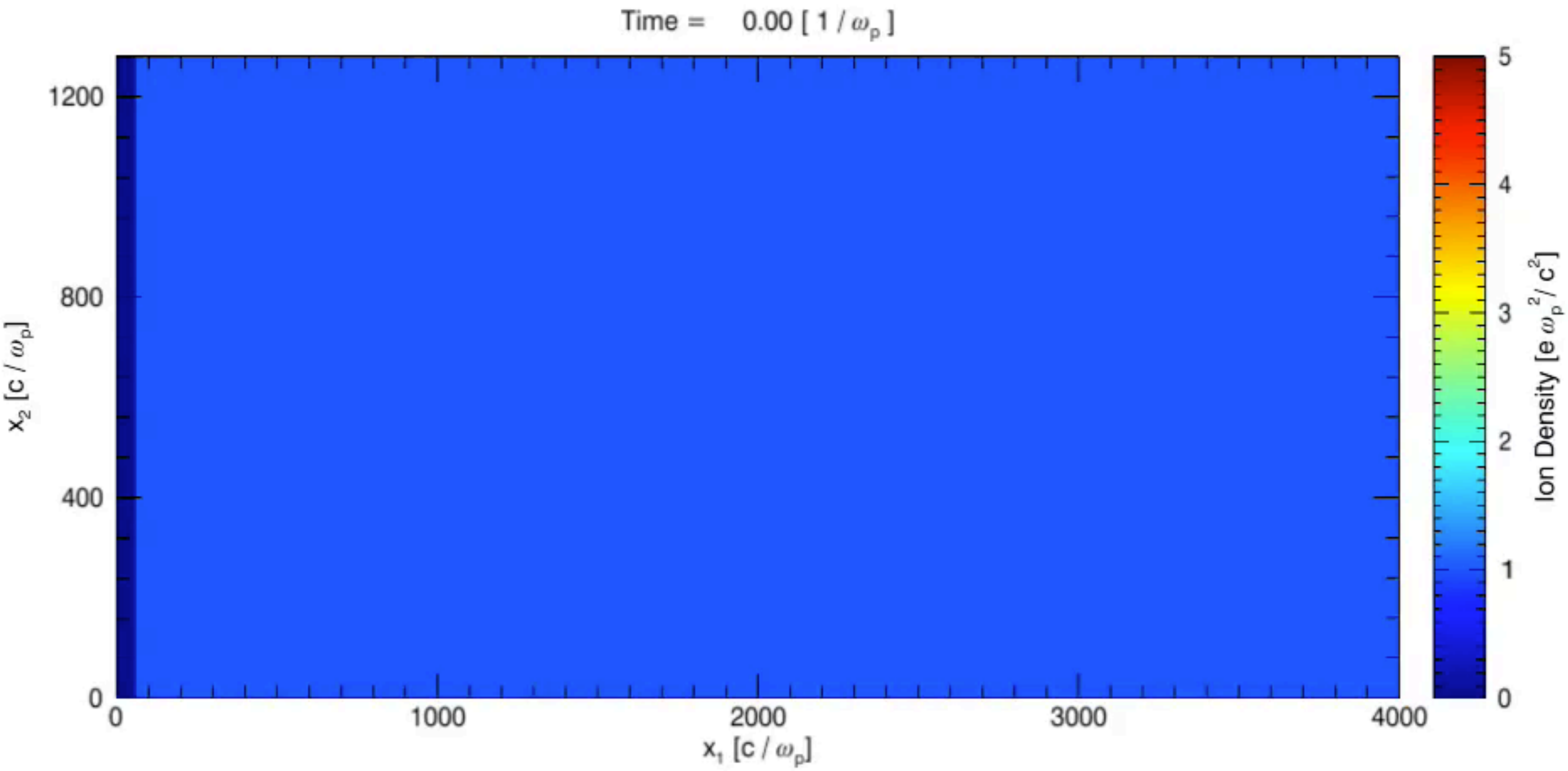

S. F. Martins *et al.*, ApJ Lett (2009)

Strong shock structure and jump conditions verified

Ion density and shock profile

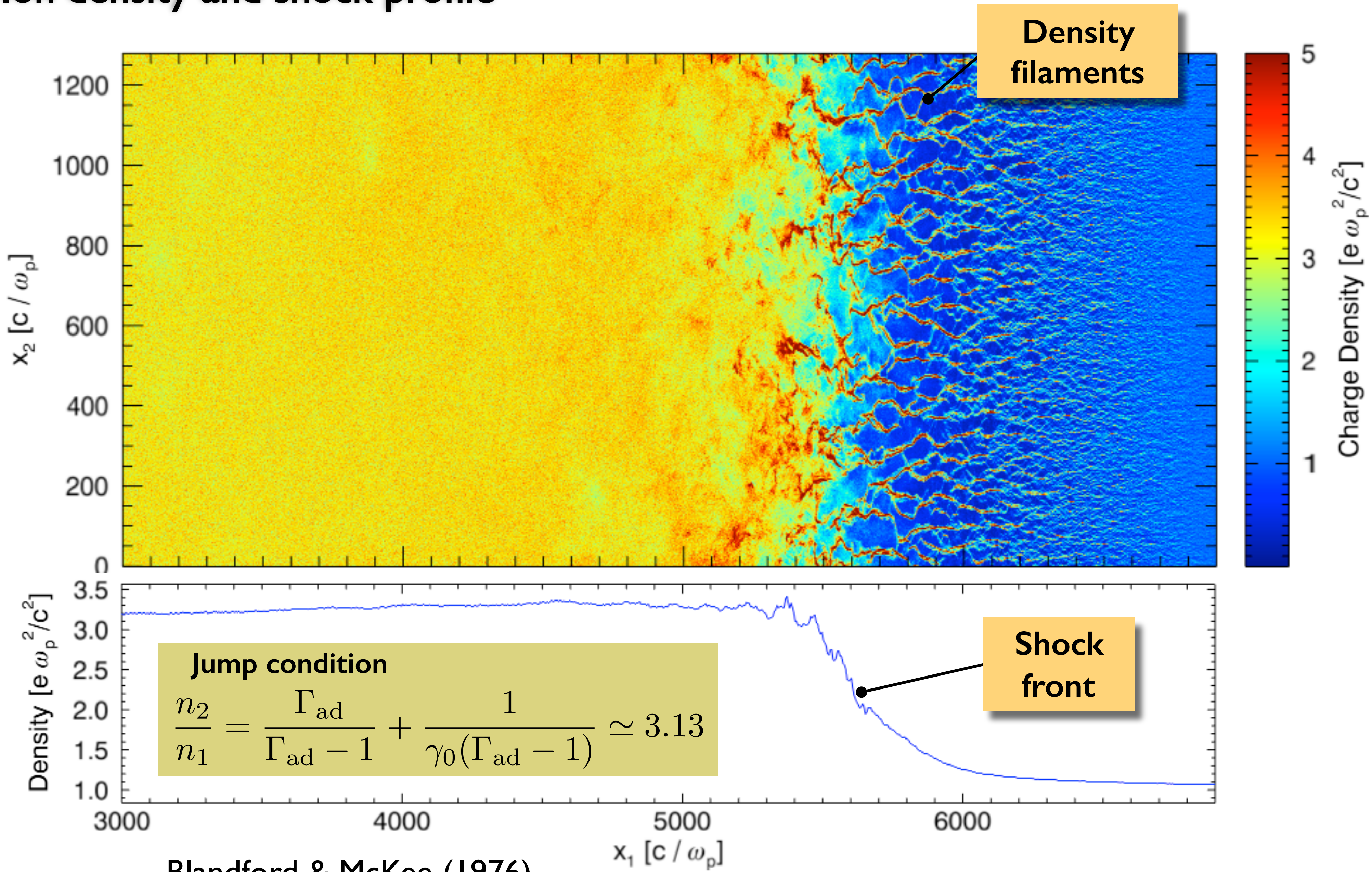

Jump condition

$$\frac{n_2}{n_1} = \frac{\Gamma_{\rm ad}}{\Gamma_{\rm ad}-1} + \frac{1}{\gamma_0(\Gamma_{\rm ad}-1)} \simeq 3.13$$

Blandford & McKee (1976)

- *Ab initio* **Fermi acceleration** determined by structure of the fields in the shock front
  [Spitkovsky 08, Martins et al, 09]

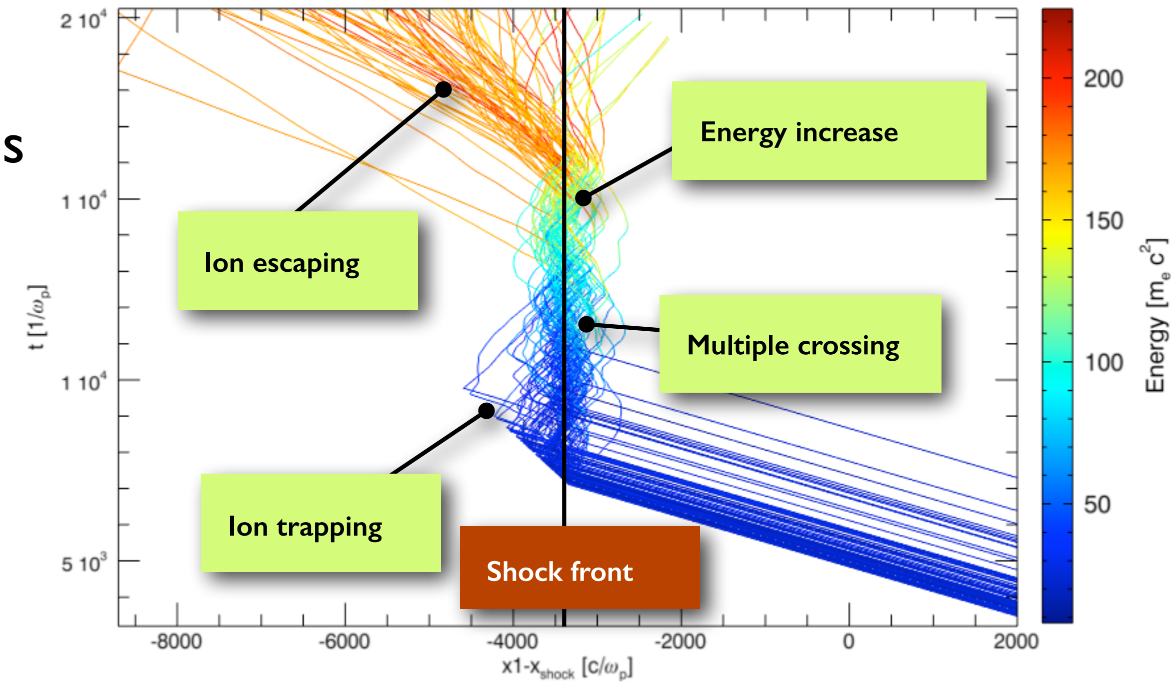

- **B-field amplification in upstream region via non-resonant "Bell" instability** [Bell 04]

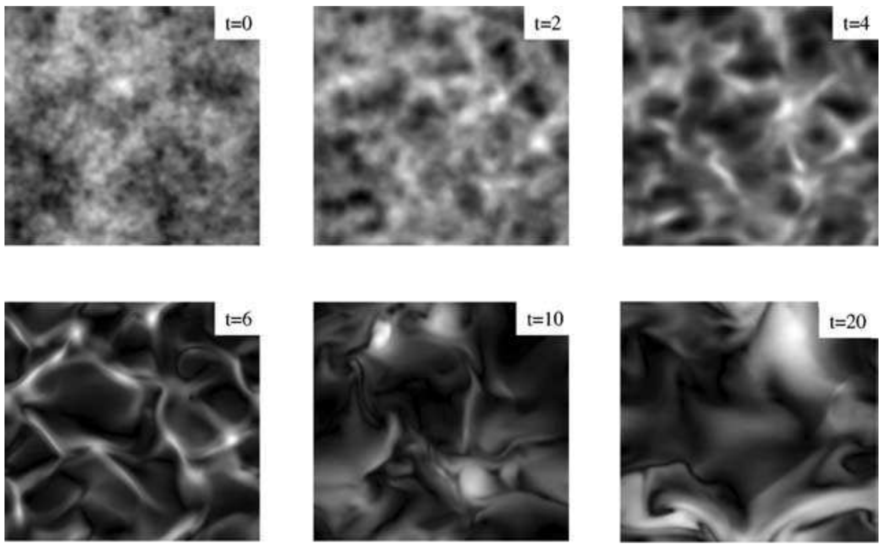

Long time evolution of the Weibel/ current filamentation instability: revisiting M. Medvedev *et al.*, ApJLett 2005 (K. Schoeffler *et al.*)

Connection with other B-field generation mechanisms (e.g. Biermann battery):
K. Schoeffler *et al.*, PRL 2014

Filaments are stable over many plasma periods in electron-proton interpenetrating flows

Electron-positron

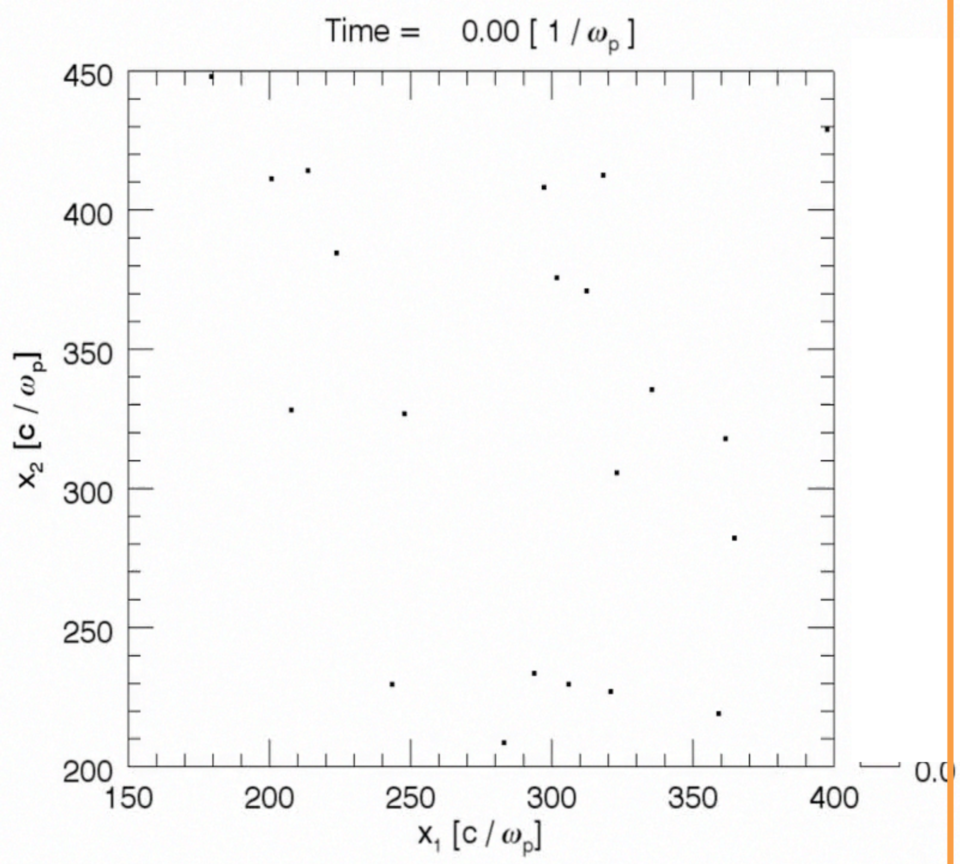

Electron-proton

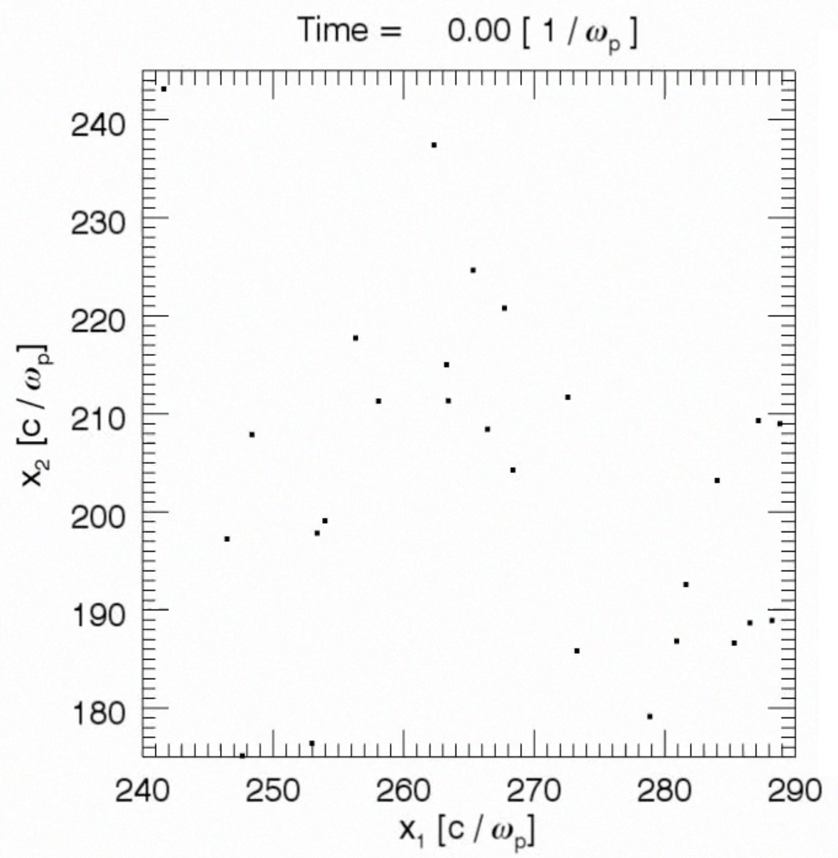

Electron trajectories follow the ExB drift in electron-ion magnetised flows

Unmagnetized scenarios

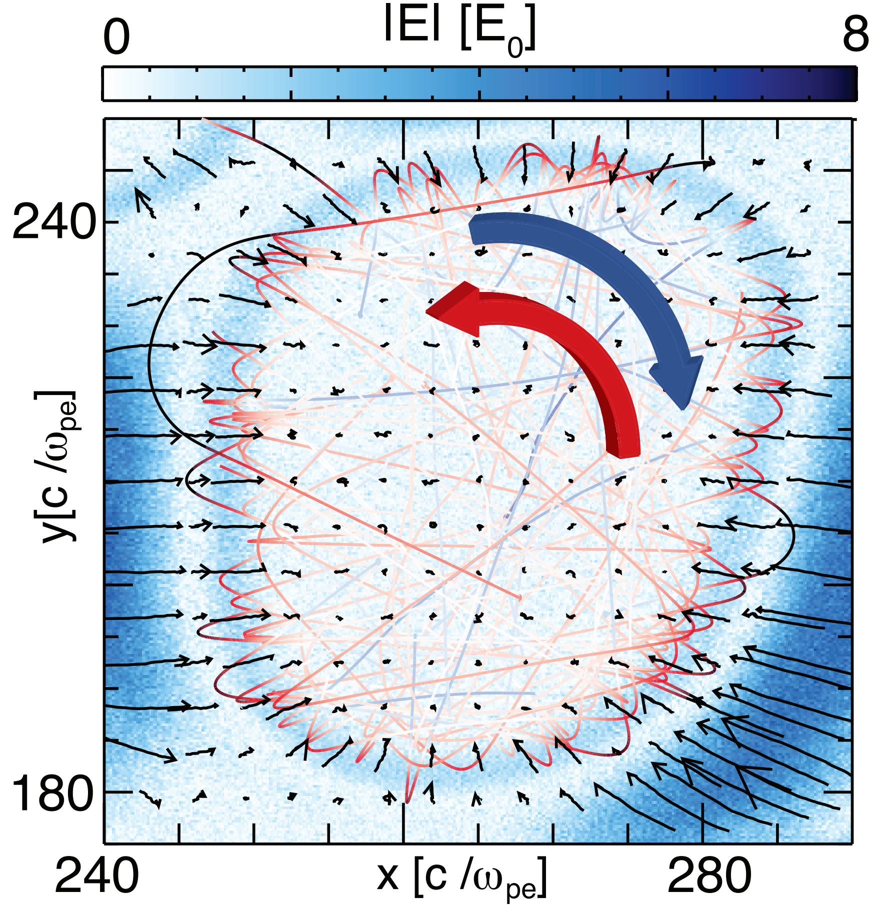

No preferential velocity direction

Magnetized

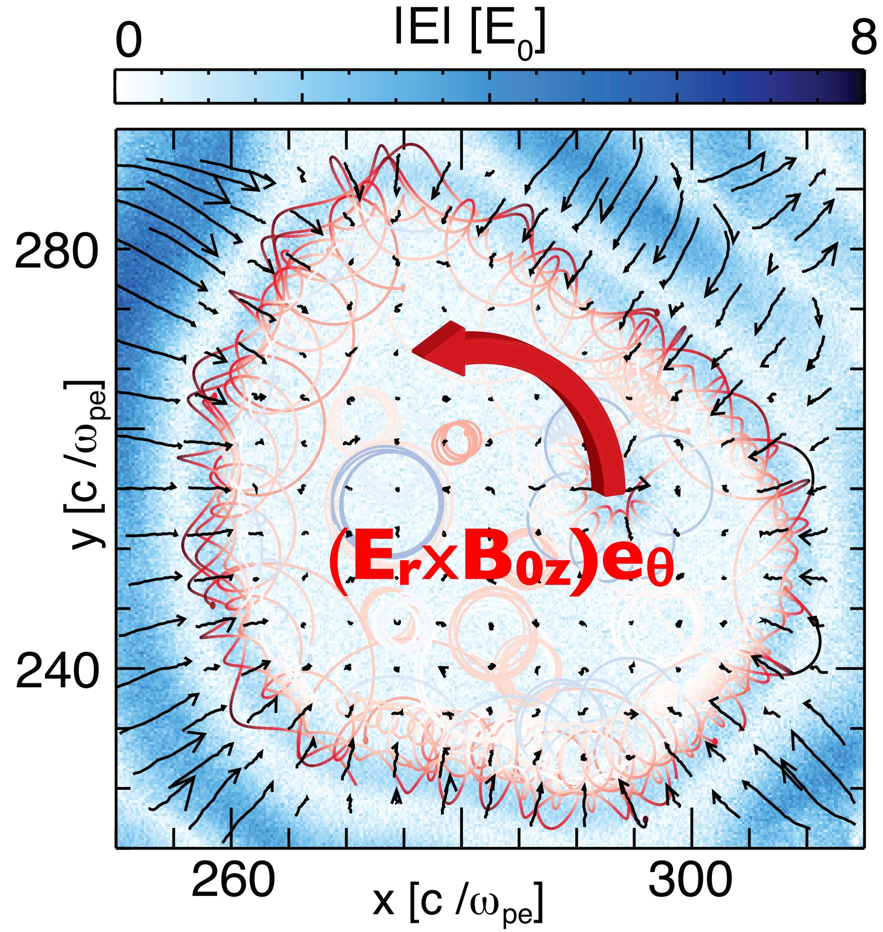

e- rotation due to ExB drift

Calculating the radiation spectrum (and polarisation)

Energy deposition pattern and spectral features

Spectrum

$$\frac{d^2 I}{d\omega dS} = \frac{e^2}{4\pi c}\left| \int_{-\infty}^{-\infty} \frac{\vec{n}\times[(\vec{n}-\vec{\beta})\times\dot{\vec{\beta}}]}{(1-\vec{n}\cdot\vec{\beta})^2 R(t')^2} e^{i\omega(t'+R(t')/c)} dt \right|^2$$

Power

$$\frac{dP}{dS} = \frac{e^2}{4\pi c}\frac{|\vec{n}\times[(\vec{n}-\vec{\beta})\times\dot{\vec{\beta}}]|^2}{(1-\vec{\beta}.\vec{n})^5 R(t')^2}$$

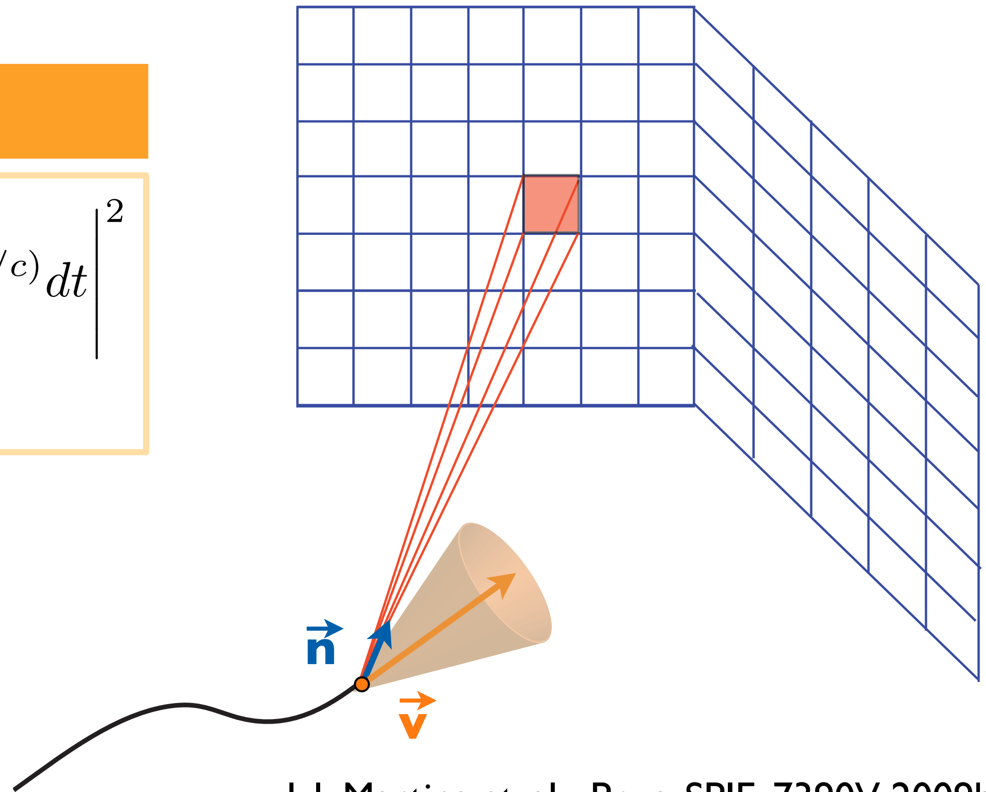

J. L.Martins et. al. , Proc. SPIE, 7390V, 2009b

Degree of Circular Polarization

$$P_c = s_3/s_0; \quad s_3 = 2Im\left\langle E_x E_y^* \right\rangle; \quad s_0 = |E_x|^2 + |E_y|^2$$

$P_c = \quad 1$ RCP

$= -1$

CP photon flux

$$\left\langle P_c \right\rangle_\omega = \frac{\int P_c I_{rad} d\omega}{\int I_{rad} d\omega}$$

$$\left\langle P_c \right\rangle = \frac{\iint P_c I_{rad} d\omega dS}{I_{rad} d\omega dS}$$

Polarization depends on magnetization (external B field) in current filamentation instability

Finite circular polarisation

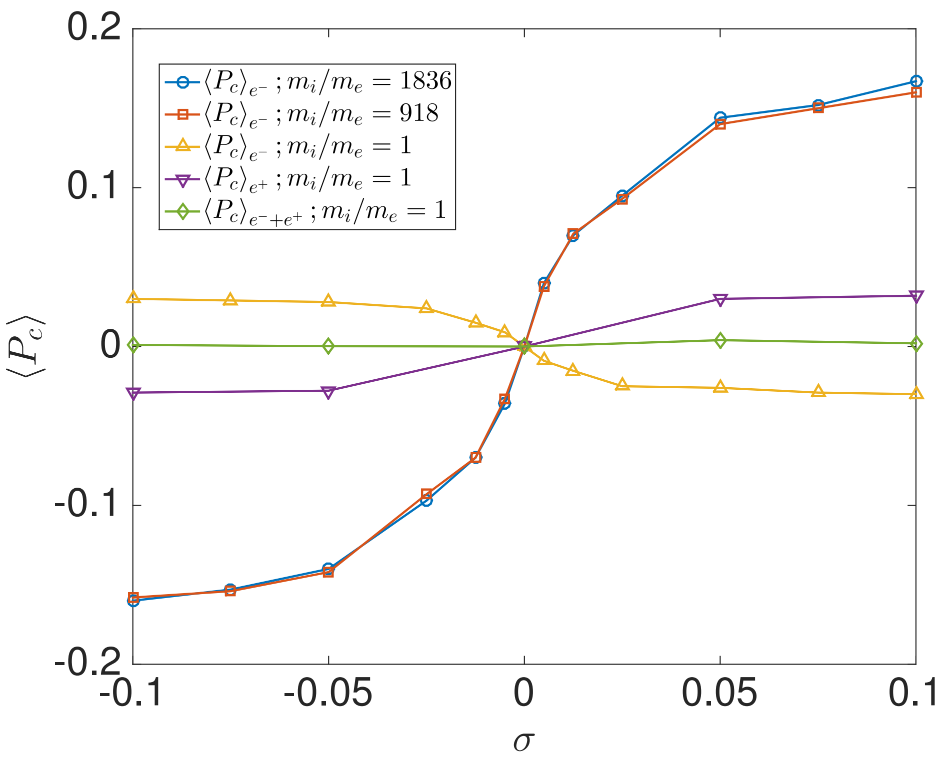

Magnetisation ($\sigma \propto B_0^2/\gamma_0$)

Onset of circular polarisation

Mass ratio

- $m_i/m_e \gg 1$
- Electron motion much faster than filament merging time

Magnetic fields

Weak magnetisations ($\sigma \ll 1$) yield 10-20% circularly polarised x-rays

Multiple sources

No influence on final polarisation (random phase approximation)

Outline

Particle in cell simulations towards the exascale

Laser particle acceleration and exotic beams

Exploring fundamental plasma processes for lab and astro

Moving to ultra high intensities

http://epp.ist.utl.pt/

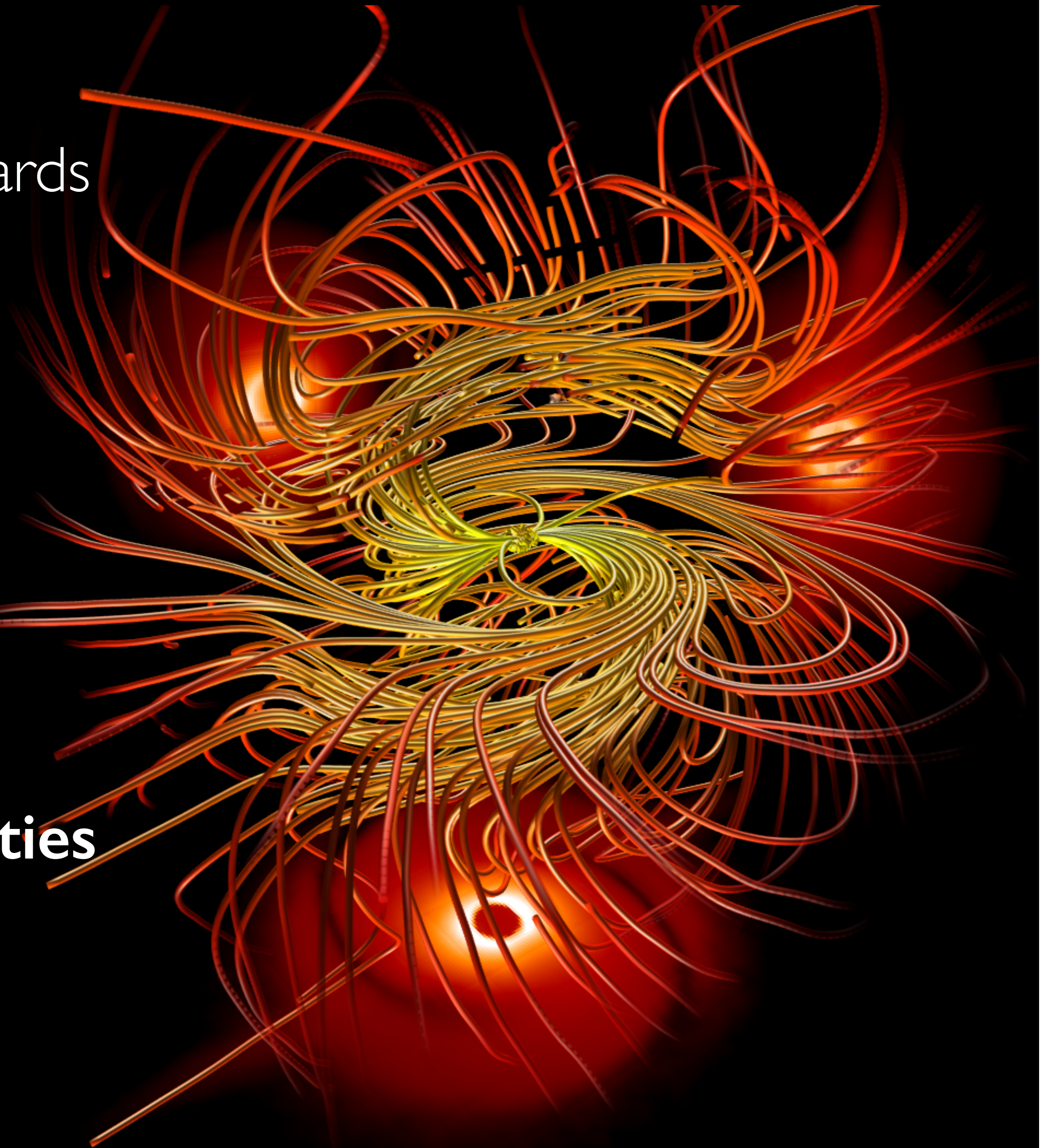

All-optical radiation reaction configuration

Identifying radiation reaction signatures in electron beam spectrum

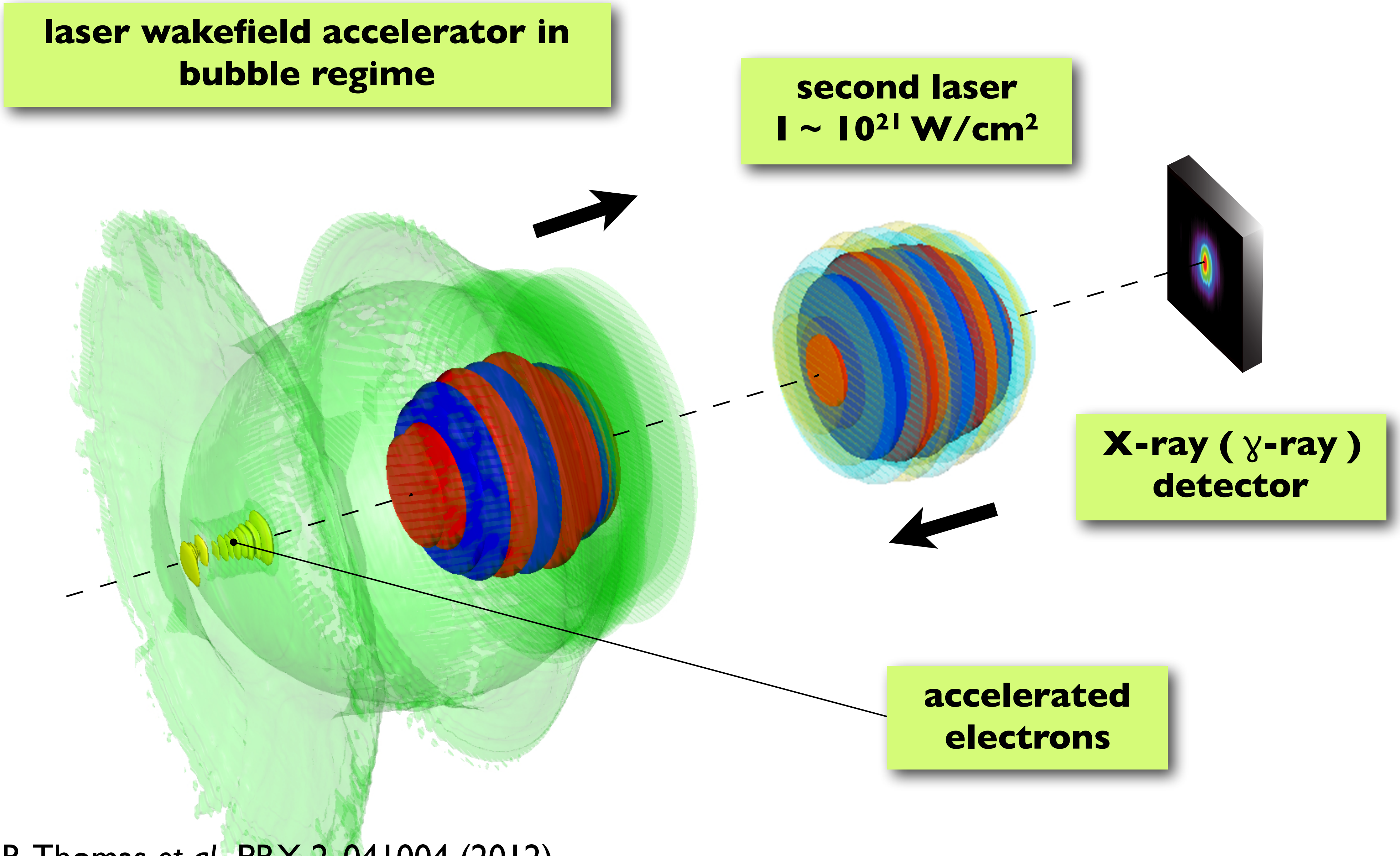

A. G. R. Thomas *et al.*, PRX 2, 041004 (2012)
M. Vranic *et al.*, PRL 113, 1348001(2014)

~40% energy loss for 1 GeV beam at 10^{21} W/cm^2

Radiation reaction can be tested with state-of-the-art lasers in this configuration

3D full-scale parameter scan

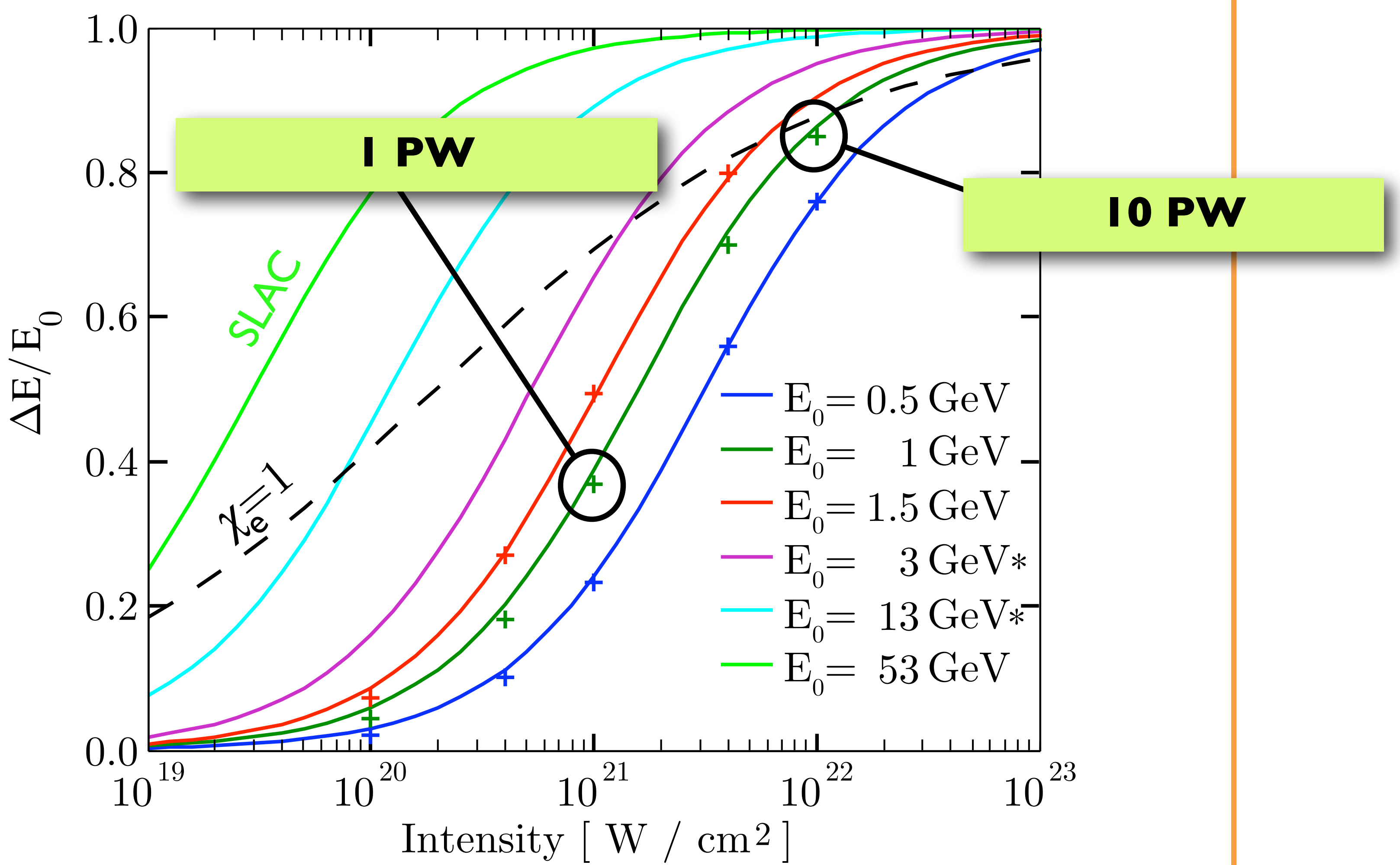

M.Vranic *et al.*, PRL 113, 1348001(2014)

Pairs can be produced already at $\chi = 0.6$

~ 200 pairs obtained per 1 000 000 interacting electrons

Parameters

laser $I \sim 2\text{x}10^{21}$ W/cm^2, 30 fs, 800 nm
electron initial energy ~ 3 GeV

electron
positron
photon

interacting laser

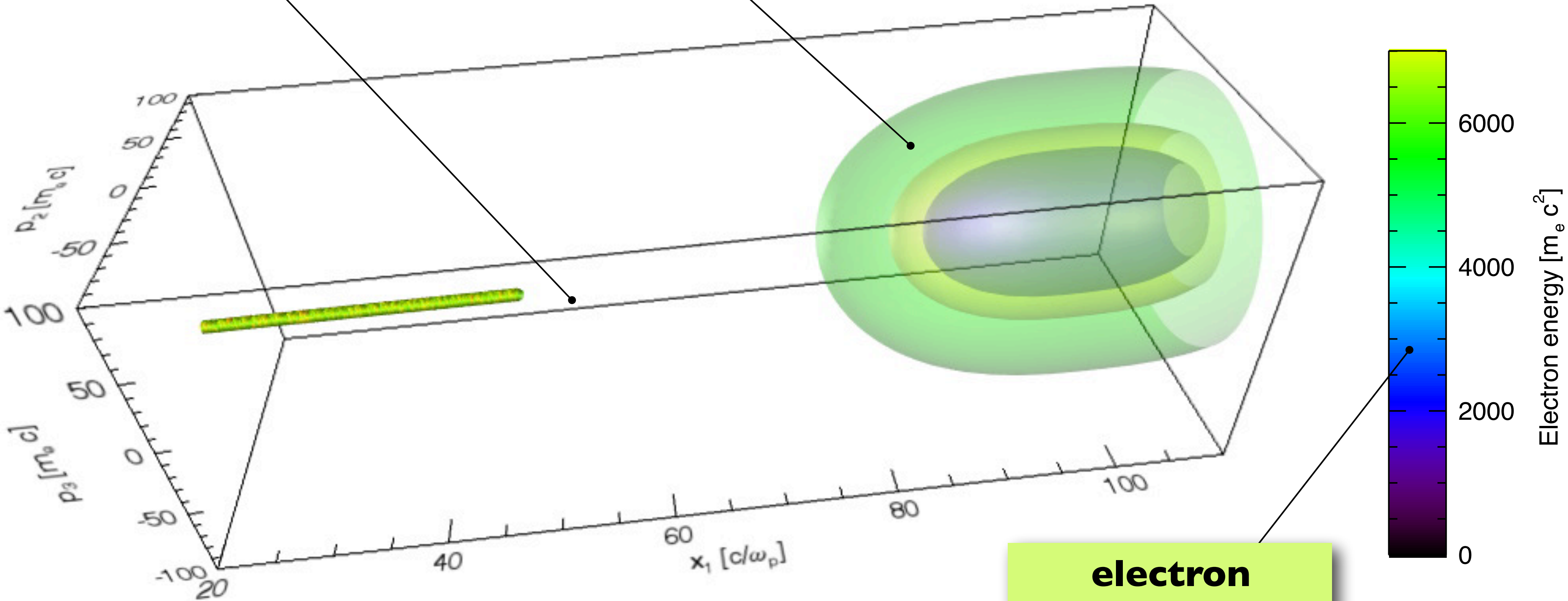

electron energy

Electron beam energy spread and divergence:
M.Vranic *et al.*, NJP (2016); ArXiv1511.04406

Capturing QED in PIC codes

2009 | 2010 | 2011 | 2012

Monte Carlo simulations showing pair production *via* real photons per electron

J. G. Kirk, A. R. Bell, and I. Arka, PPCF 51, 085008 (2009).

R. Duclous, J.G. Kirk & A.R. Bell, PPCF, 53, 015009 (2010)

PIC simulations of QED cascade in various configuration (counter propagating laser, rotating field)

N.V. Elkina et al, Phys. Rev. ST. AB., 14, 054401 (2011)

E.N. Nerush, et al, Phys. Rev. Lett., 106, 035001 (2011)

Dense pair Plasmas and Ultra-Intense Bursts of Gamma-Rays from Laser-Irradiated Solids

C.P. Ridgers, et al Phys. Rev.Lett., 108, 165006 (2012)

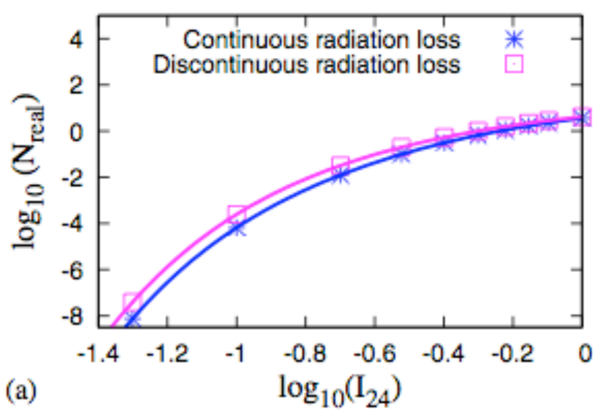

Number of pairs produced

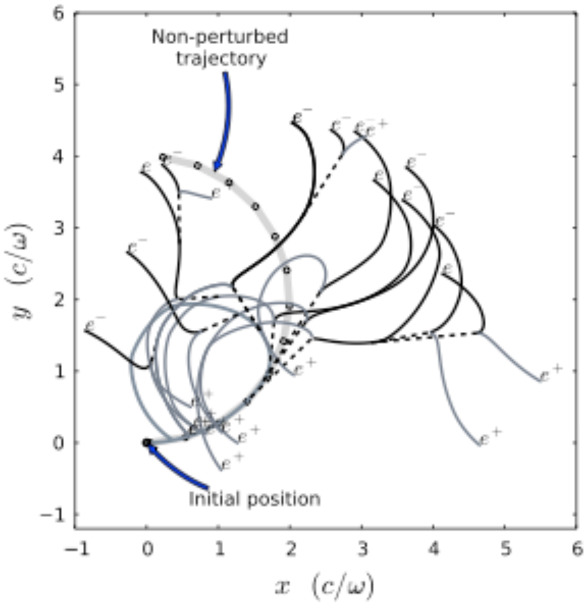

Picture of a cascade in rotating field

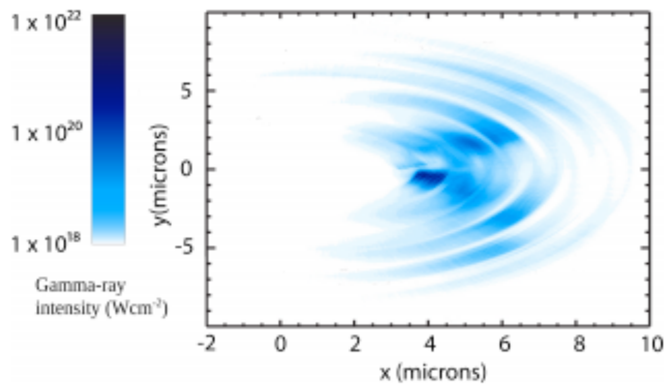

Gamma rays from laser-irradiated solid

Modelling of QED cascades (& radiation cooling)

T. Grismayer *et al.*

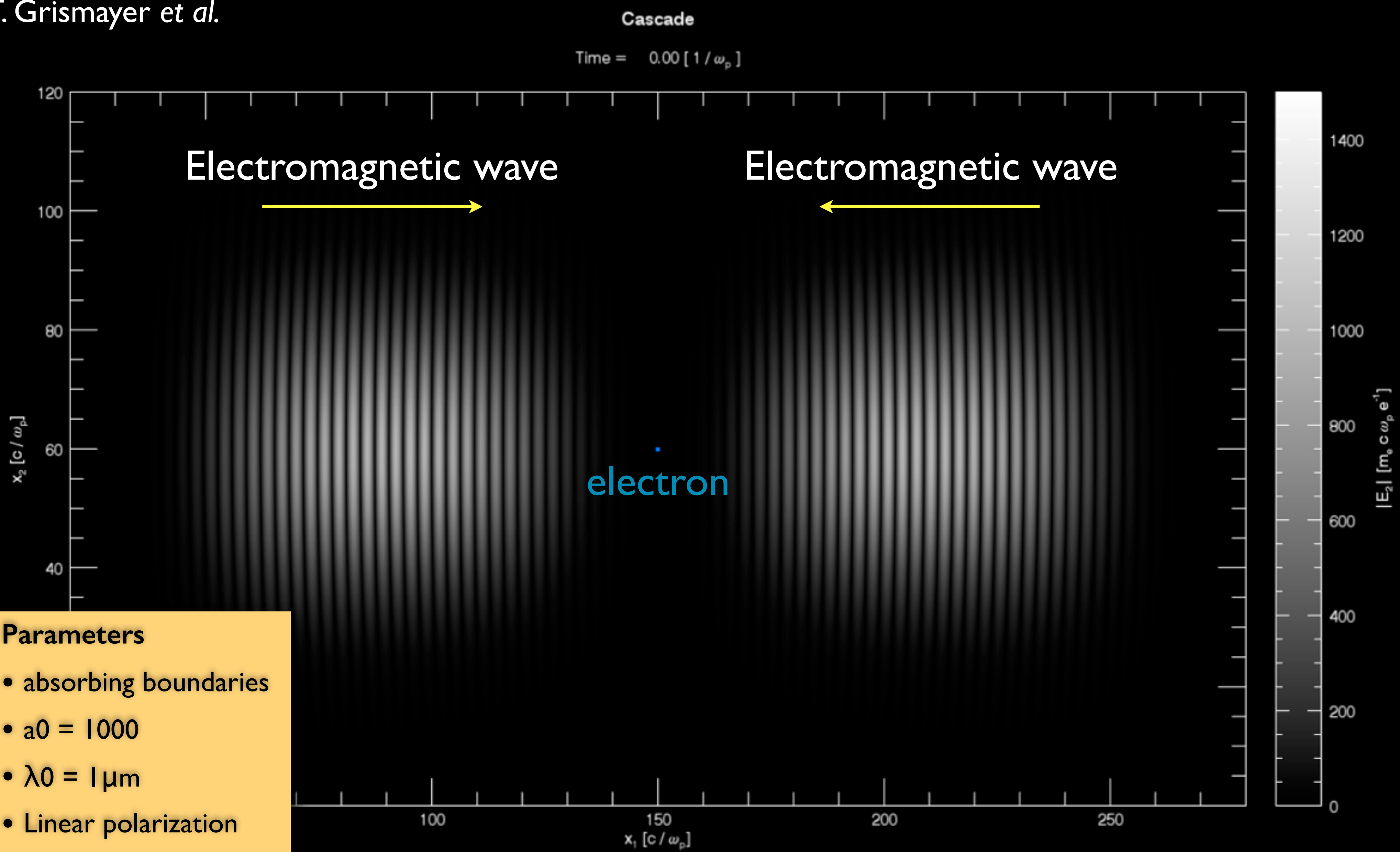

Parameters

- absorbing boundaries
- a0 = 1000
- λ0 = 1 μm
- Linear polarization
- W0 = 5 μm
- τ = 30 fs

QED cascades in counter propagating electromagnetic fields

T. Grismayer *et al.*

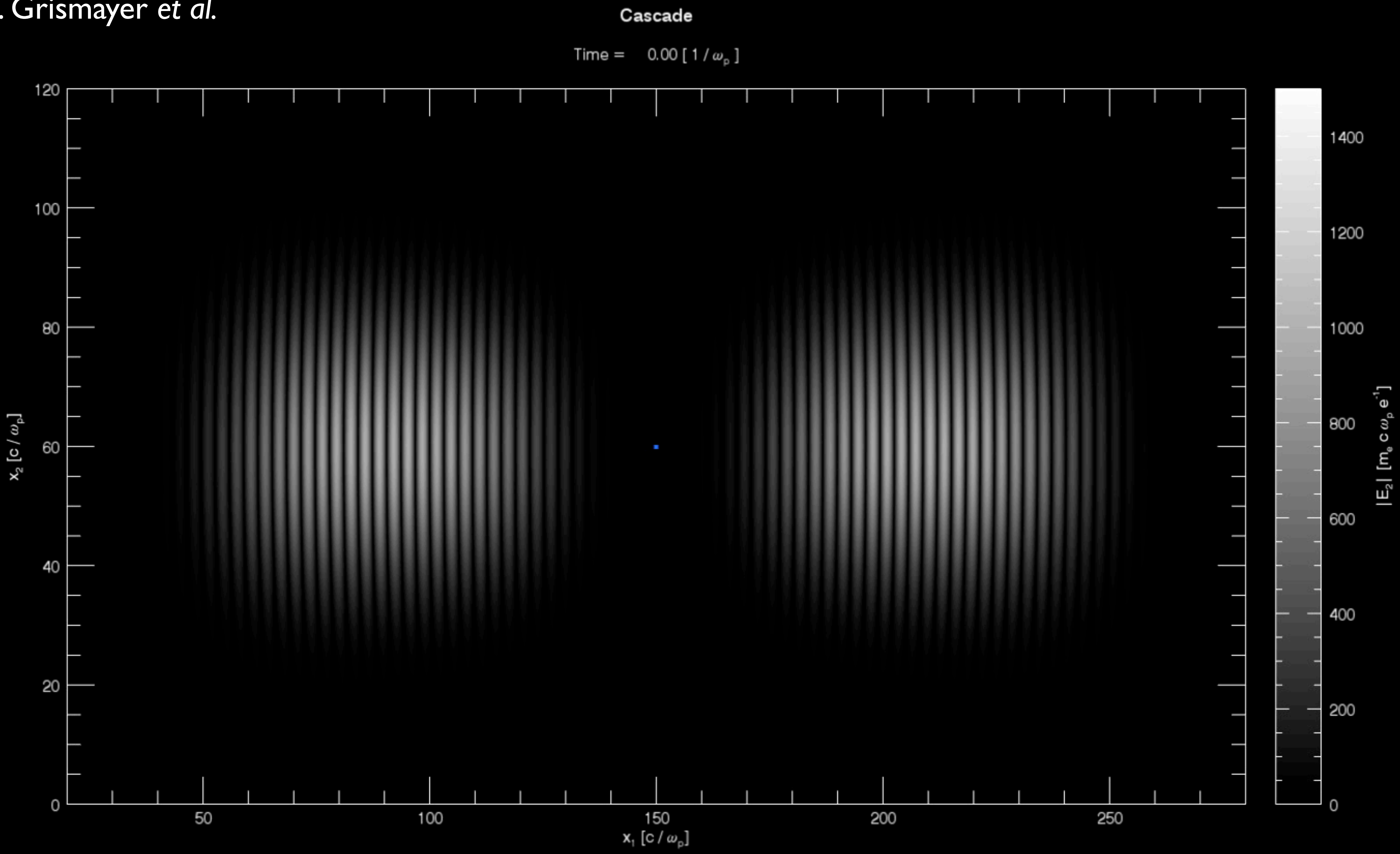

photons positron electron

Optimal QED configurations with standing waves

This requires finding where the parameter $\chi = \frac{1}{E_S}\sqrt{\left(\gamma \mathbf{E} + \frac{\mathbf{p}}{mc}\times \mathbf{B}\right)^2 - \left(\frac{\mathbf{p}}{mc}\cdot \mathbf{E}\right)^2}$ reaches high values

Linear

- electron
- positron

Parameters

- absorbing boundaries
- a0 = 1000
- λ0 = 1μm
- W0 = 5 μm
- τ = 30 fs

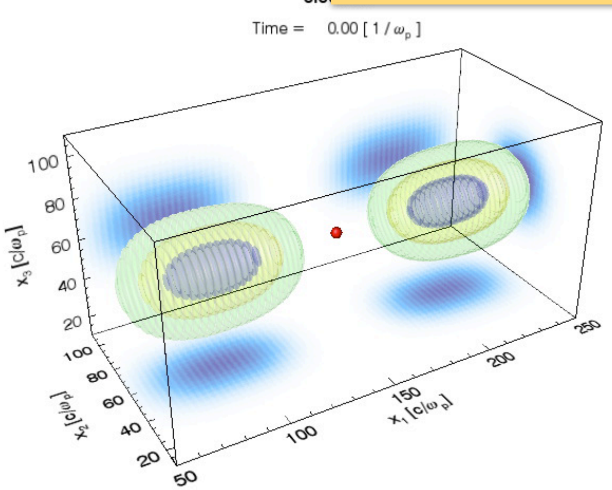

Particles remain in the x_1-x_2 plane

Double clockwise

- electron
- positron
- photon

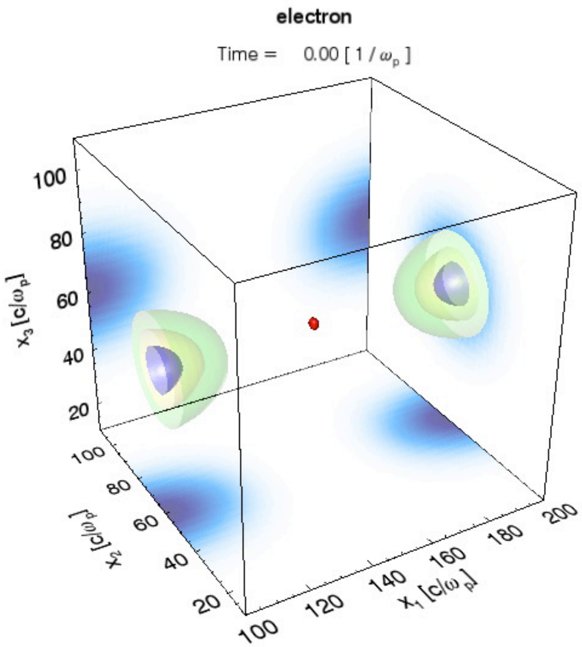

Particles explore the whole space

Clockwise-anti clockwise

- electron
- positron
- photon

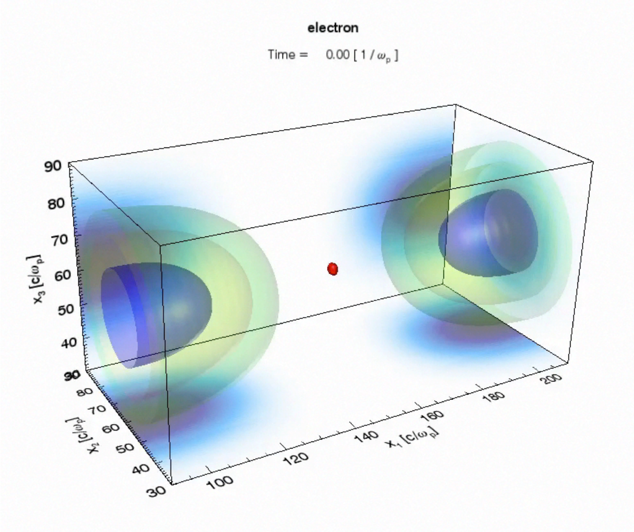

Particles rotate mainly in the x_2-x_3 plane

T. Grismayer *et al.*, APS DPP, 2013
T. Grismayer *et al.*, to appear 2016

QED cascades: from the seed to full laser absorption

Analytical growth rate model + 3D full scale parameter scan

T. Grismayer, *et al.*, ArXiv: 1511.07503

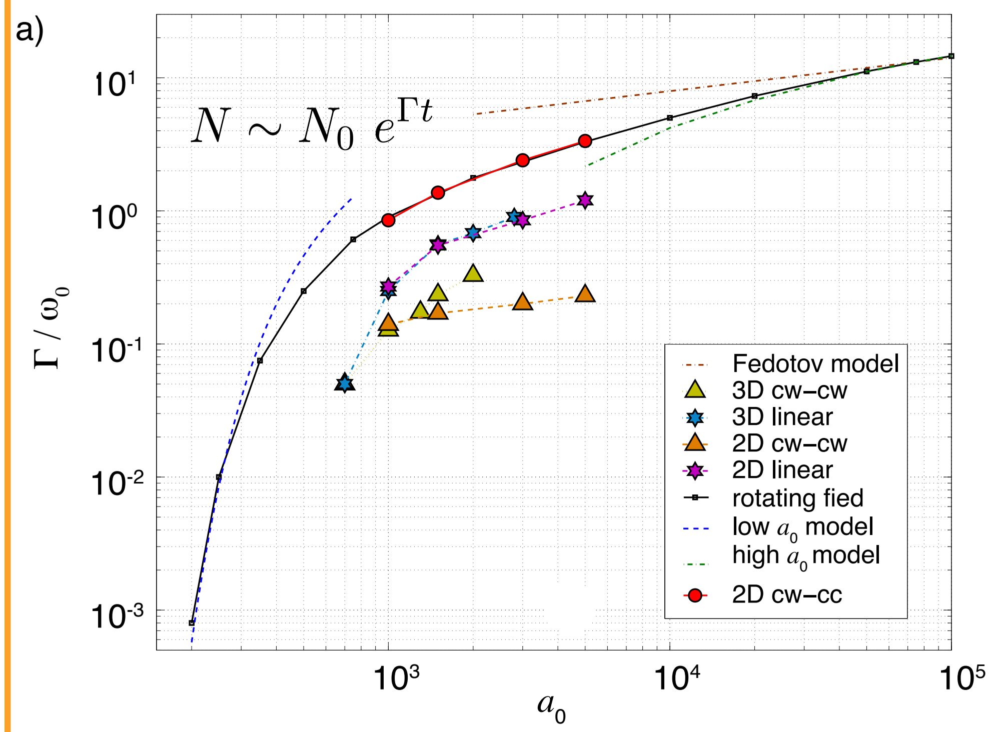

Laser absorption via QED cascades absorption model + 2D/3D simulations

T. Grismayer, *et al.*, PoP (2016); ArXiv: 1512.05174

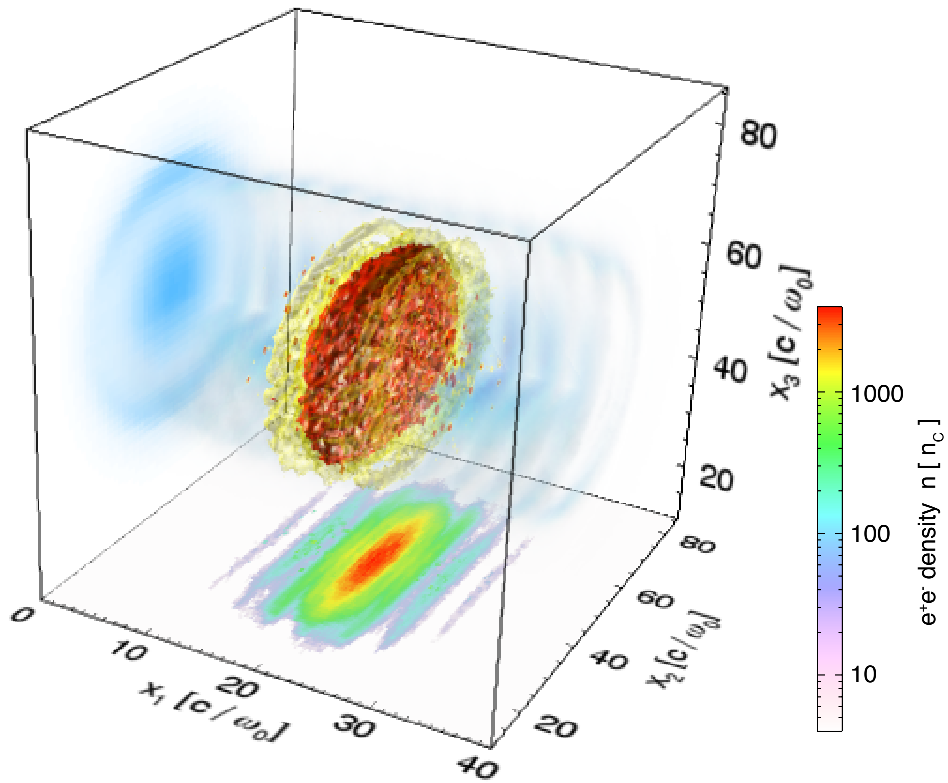

Possibility to achieve conditions close to the Goldreich-Julian density e-e+ density ~ n_{cr} ~ Goldreich-Julian density
A. Gruzinov, Arxiv:1404.4615v1 (2014)

Heisenberg-Euler QED corrections

Physics below Schwinger limit

Relevance for extreme astrophysical scenarios?

Effect on laser properties as we reach Schwinger limit?

Extract observable consequences of QED predictions.

Multi PW lasers combined with x-ray lasers will allow us to probe the dynamics of the Quantum Vacuum.

Heisenberg-Euler corrections to Maxwell's Equations*

Electron-positron fluctuations give rise to an effective polarisation and magnetisation of the vacuum which can be treated in an effective form as corrections to Maxwell's equations.

$$\mathcal{L} = \boxed{\mathcal{L}_{\mathcal{M}} + \mathcal{L}_{HE}} + \mathcal{L}_D$$

Valid for static inhomogeneous fields such that

$$E << E_S \qquad \omega << \omega_c$$

$$E_S = \frac{m^2 c^3}{e\hbar} \qquad \omega_c = \frac{mc^2}{2\hbar}$$

Effectively, we obtain a highly non linear, non dispersive vacuum (e.g. M.Soljačić and M. Segev Phys. Rev. A 62, 043817 (2000))

Higher order corrections include spatial and temporal derivatives of these corrections. May be neglected for:

$$\omega << \omega_c \frac{E}{E_S}$$

*W. Heisenberg and H. Euler, Z. Physik 98, 714 (1936).

Heisenberg-Euler QED corrections

Quantum vacuum corrections to Maxwell's equations nonlinearly couple all field components

- Electron-positron fluctuations give rise to an effective polarisation and magnetisation of the vacuum which can be treated in an effective form as corrections to Maxwell's equations*.

$$\frac{\partial \vec{B}}{\partial t} + \vec{\nabla} \times \vec{E} = 0 \qquad \vec{\nabla} \cdot B = 0$$

$$\vec{\nabla} \times \vec{H} - \frac{\partial \vec{D}}{\partial t} = 0 \qquad \vec{\nabla} \cdot D = 0$$

- with the constitutive relations,

$$\vec{D} = \varepsilon_0 \vec{E} + \vec{P} \qquad \vec{B} = \mu_0 \vec{H} + \vec{M}$$

$$\vec{P} = 2\xi \left[2(E^2 - c^2 B^2)\vec{E} + 7(\vec{E} \cdot \vec{B})\vec{B} \right]$$

$$\vec{M} = -2\xi \left[(2(E^2 - c^2 B^2)\vec{B} - 7(\vec{E} \cdot \vec{B})\vec{E} \right]$$

$$\xi = \frac{20\alpha^2 \varepsilon_0^2 \hbar^3}{45 m_e^4 c^5} \sim 10^{-51} \; [\mathrm{Fm/V^2}]$$

Effects of the quantum vacuum below the Schwinger limit

- **Relevance for extreme astrophysical scenarios?**

J.Pétri, Mon. Not. Roy. Astron. Soc (2015)

- **Unprecedented intensities will allow to probe the quantum vacuum.**
  What laser properties will be affected?

A. Di Piazza et.al, Rev. Mod. Phys. 84, 1177–1228 (2012).

- **Extract observable consequences of fundamental QED predictions.**

*W. Heisenberg and H. Euler, Z. Physik 98, 714 (1936).

Ellipticity induced in x-ray probe propagating through birefringent vacuum

T. Grismayer *et al.*

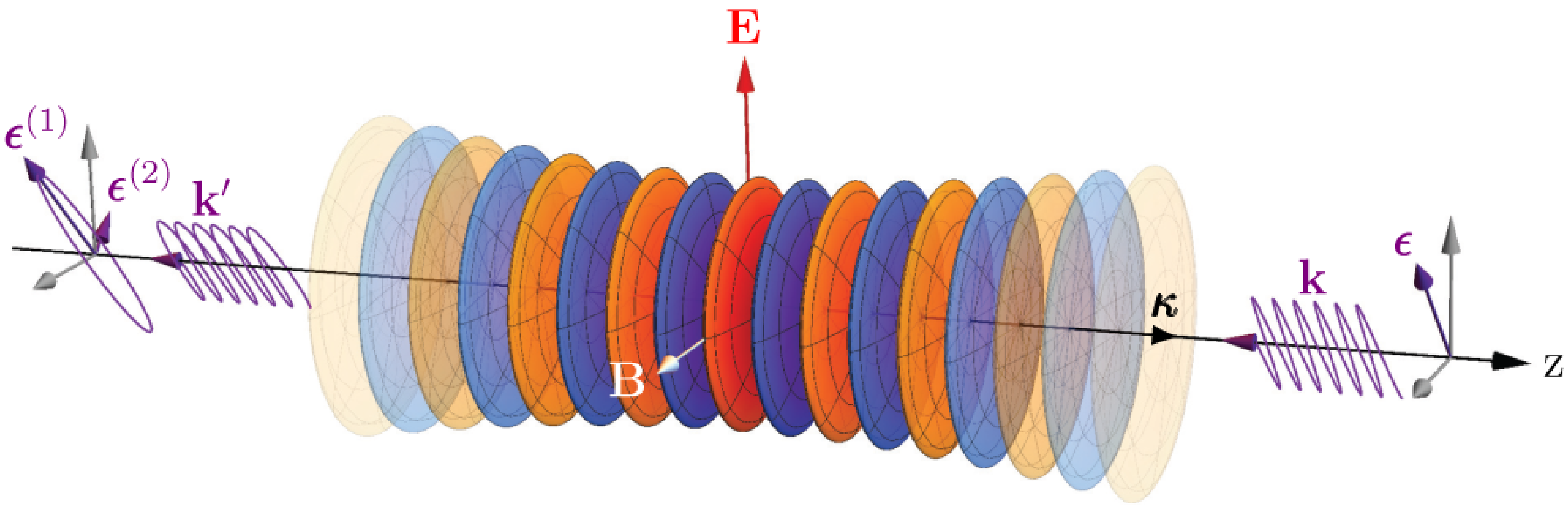

*Courtesy of Karbstein, *et al.*, PRD **92,** 071301(R) (2015).

Simulation setup*: x-ray pulse probes birefringent vacuum created by optical laser. A measurement of ellipticity induced is a direct test of the Quantum vacuum

Using our QED solver, it is possible to simulate this setup in multidimensional and, via an electromagnetic treatment, obtain the ellipticity induces at various off-axis distances and for probe/pump parameters

Simulation parameters

- $\xi = 10^{-6}$
- σ = 30 fs probe duration
- 1 keV x-ray probe
- $I = 10^{23}$ W/cm^2 pump
- λ = 1µm pump

Multi mode mixing due to nonlinear vacuum corrections

To be explored *e.g.* at HIBEF (XFEL + ultra high intensity laser)

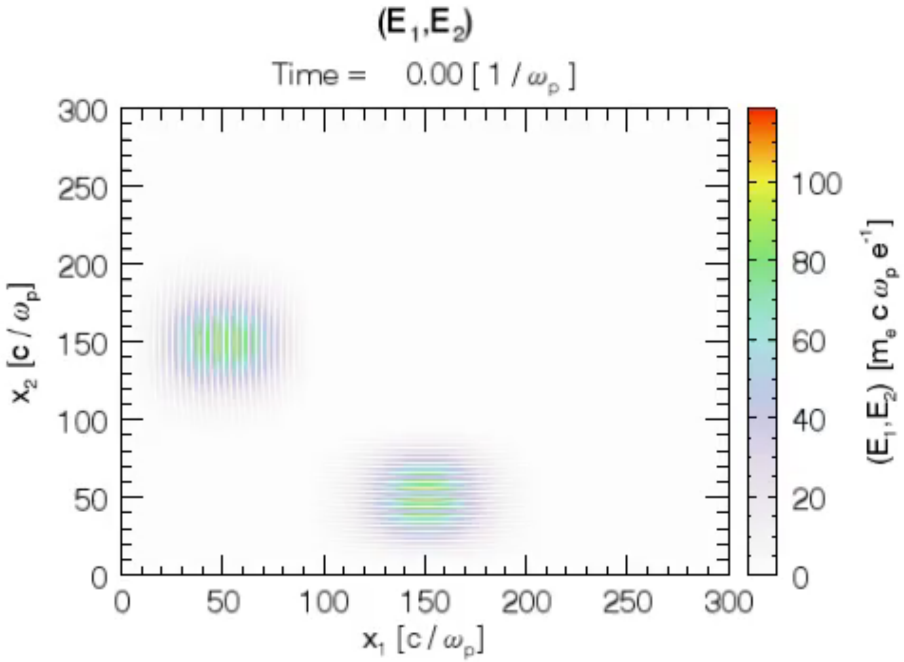

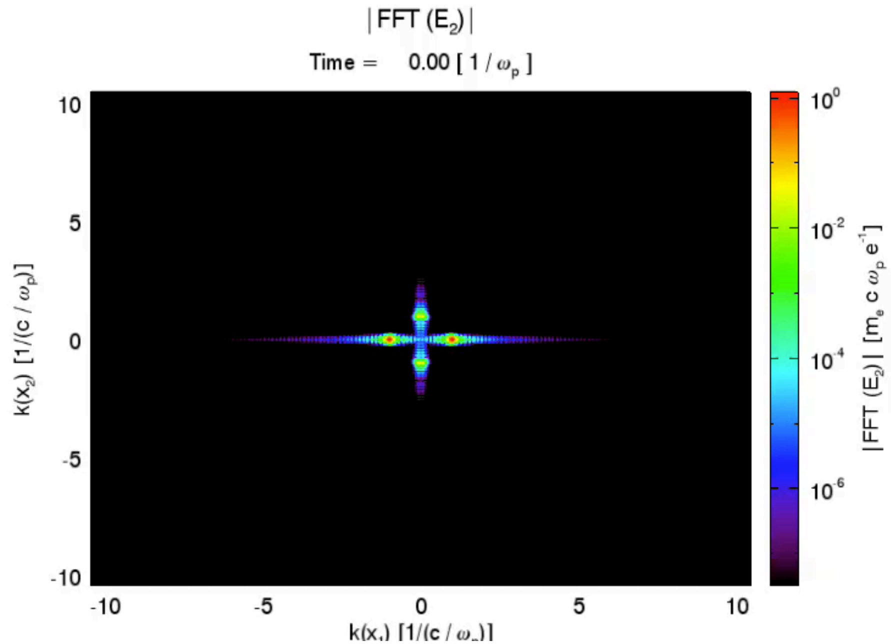

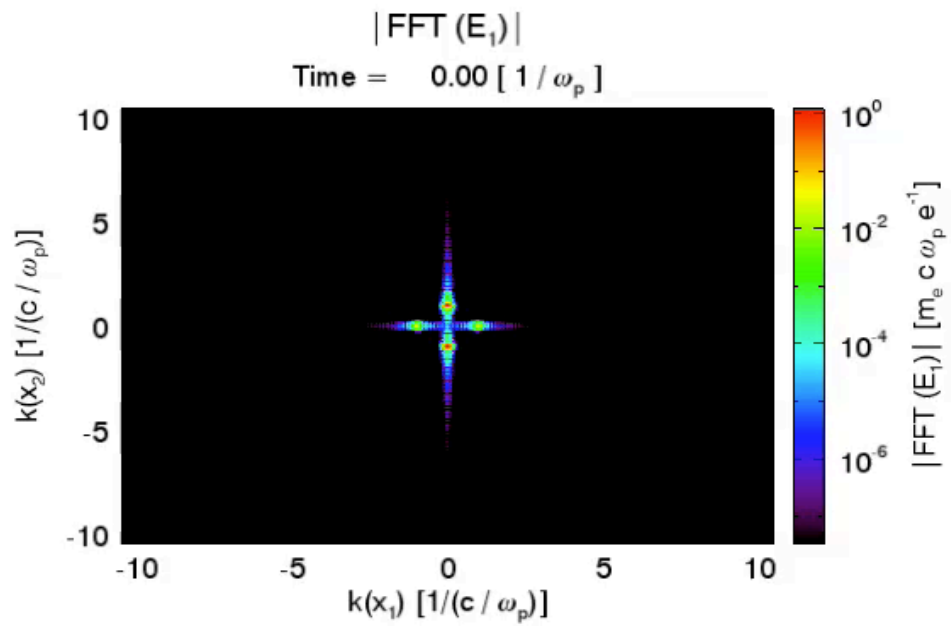

Setup with 2 Gaussian pulses propagating in perpendicular directions (a_0 = 100, ξ = $10^{-6,}$ λ = 1 μm)

Combination of odd and even harmonics is generated; **After interaction**, imprint is left in both pulses as they now freely propagate.

P. Carneiro *et al*,. arXiv:1607.04224

Outline

Particle in cell simulations towards the exascale

Laser particle acceleration and exotic beams

Exploring fundamental plasma processes for lab and astro

Moving to ultra high intensities

http://epp.ist.utl.pt/

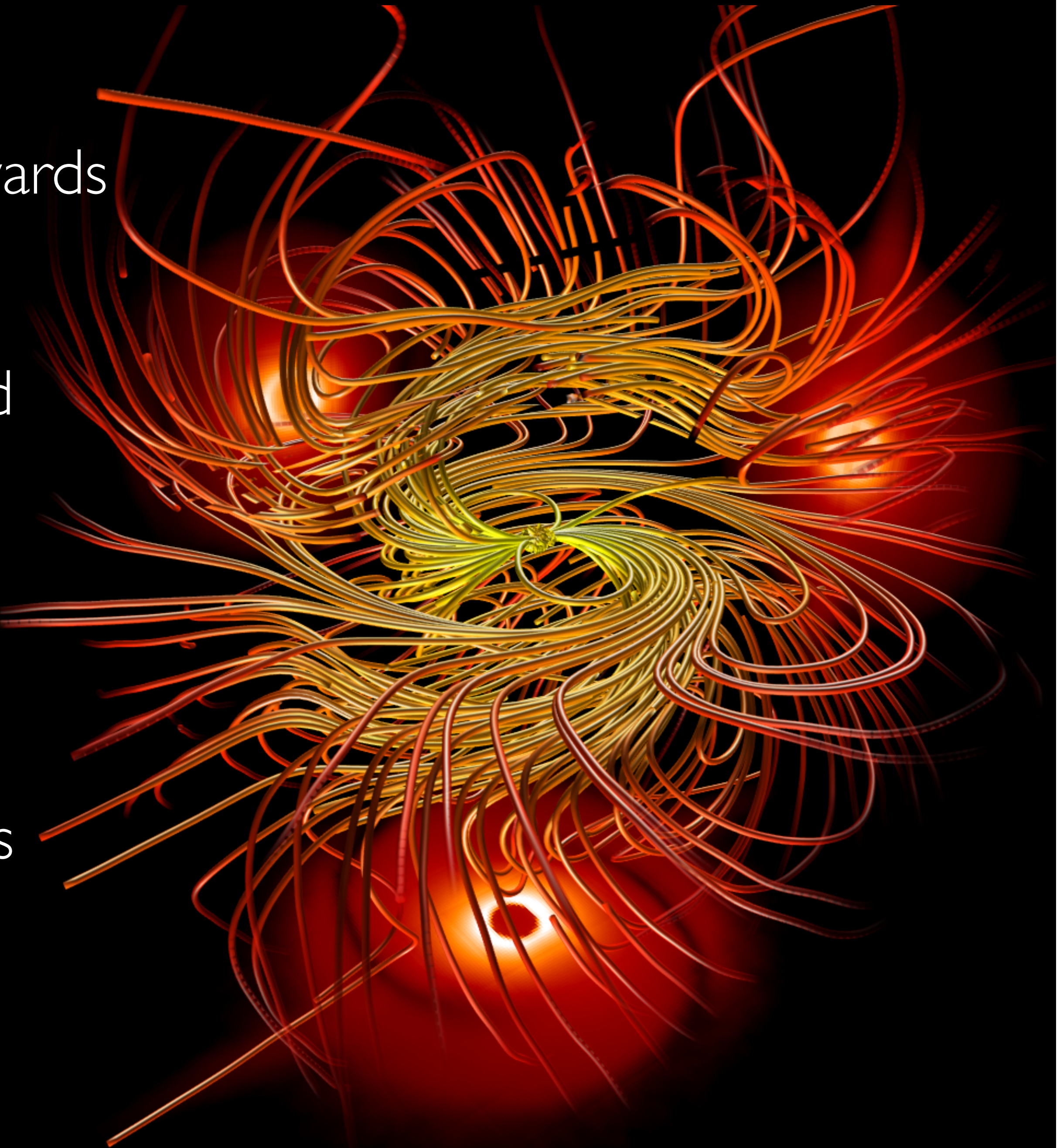

Scenarios where all this comes together

Pulsar magnetospheres…

M.A. Belyaev, MNRAS (2015); A.A Philippov, A. Spitkovsky, B. Cerruti, ApJ Lett (2015); Y. Chen, A. M. Beloborodov, ApJ Lett (2014); A.A Philippov, A. Spitkovsky, ApJ Lett (2014); A. N. Timokhin, MNRAS (2010)

JK Daugherty and AK Harding, ApJ (1982); P. Goldreich and W.H Julian, ApJ (1969)

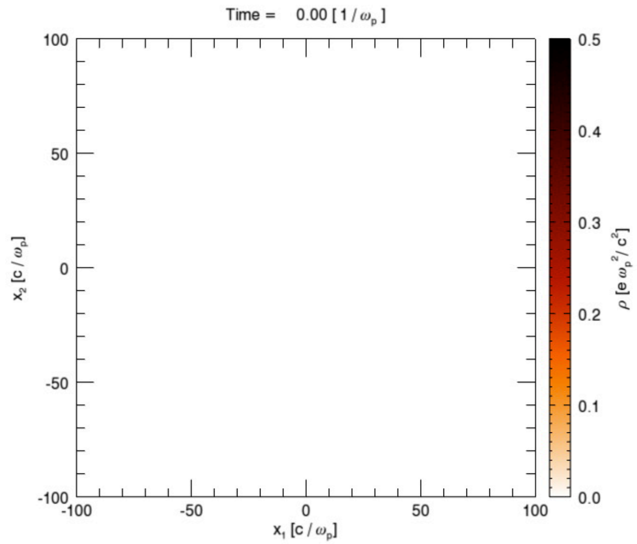

… in the laboratory?

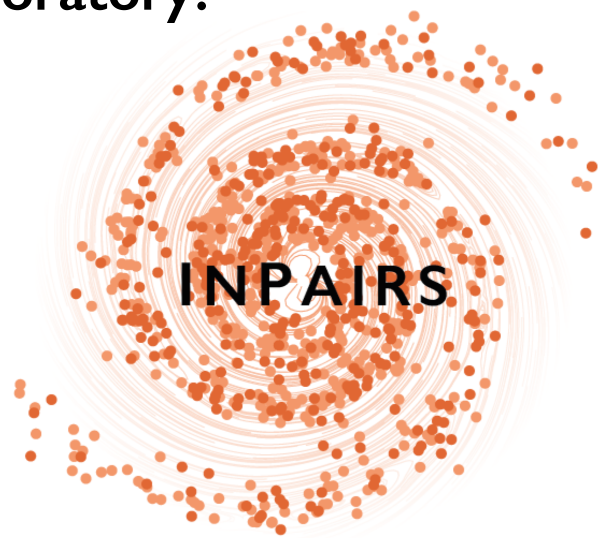

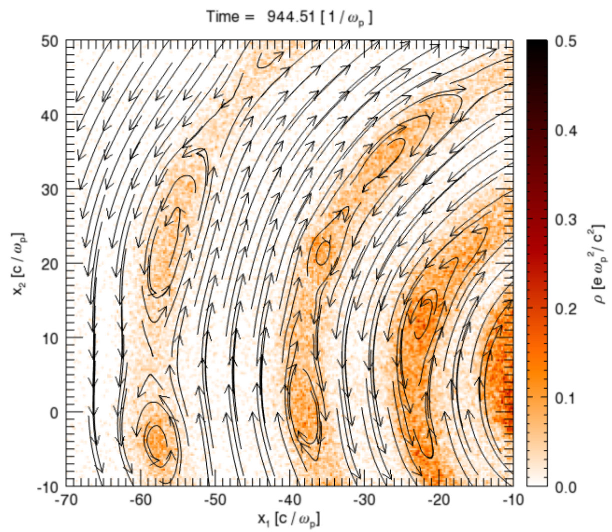

Summary

A wide range of extreme laboratory and astrophysical scenarios can now be explored and captured by *ab initio* simulations

Continuous interplay between theory, multi scale models, and outstanding computational advances will continue to drive important advances *in silico*

http://epp.ist.utl.pt/